Monofilament MgB_2 Wires for MRI Magnets

by

Jiayin Ling

Submitted to the Department of Mechanical Engineering
in partial fulfillment of the requirements for the degree of

Master of Science in Mechanical Engineering

at the

MASSACHUSETTS INSTITUTE OF TECHNOLOGY

September 2012

ARCHIVES
MASSACHUSETTS INSTITUTE OF TECHNOLOGY
OCT 2 2 2012
LIBRARIES

© Massachusetts Institute of Technology 2012. All rights reserved.

Author .....
Department of Mechanical Engineering
August 24, 2012

Certified by .....
Yukikazu Iwasa
Thesis Supervisor

Accepted by .....
David E. Hardt
Chairman, Departmental Committee on Graduate Students

Monofilament MgB_2 Wires for MRI Magnets

by

Jiayin Ling

Submitted to the Department of Mechanical Engineering
on August 24, 2012, in partial fulfillment of the
requirements for the degree of
Master of Science in Mechanical Engineering

Abstract

MRI magnets are useful medical devices in early detection and efficient treatment of disease or injury. Because of the significant better performance, MRI magnets are made of superconductors rather than made of copper. Nowadays, there are over 20,000 superconducting MRI magnets installed worldwide. Most of them are made of NbTi or Nb_3Sn, but they are usually very expensive to purchase or operate. So, my colleagues chose MgB_2 wires to develop low-cost and easy-to-operate MRI units which serve to the majority of the humanity.

Because we have a reliable technology to fabricate superconducting joints with monofilament MgB_2 wire, we decided to build our MgB_2 MRI magnet with monofilament wire instead of multifilament wire. Previously, flux jumping was found to be the main issue with monofilament superconducting wire; we have to demonstrate that flux jumping is not a big issue with monofilament MgB_2 wire before we can build our MRI magnet with it.

In this thesis, a series of experiments was designed and carried out to prove that the monofilament MgB_2 wire performs as well as the multifilament MgB_2 wire in MRI magnet applications. Short samples of monofilament MgB_2 wires were tested, and magnetization trace of the short samples showed that flux jumping could be a minor issue with monofilament MgB_2 wire. Three 100-m sample coils made of multifilament MgB_2 wire, monofilament MgB_2 wire, and monofilament NbTi wire were wound, tested and compared. The results of these tests demonstrated that the monofilament MgB_2 wire has insignificant flux jumping which does not lead to a premature quench. So, monofilament MgB_2 wire is potentially a good option for MRI magnets.

Thesis Supervisor: Dr. Yukikazu Iwasa
Title: Head and Research Professor, Magnet Technology Division, Francis Bitter Magnet Laboratory

Acknowledgments

First and foremost, I would like to thank my advisor, Dr. Yukikazu Iwasa. Dr. Iwasa is not only a superb expert in superconducting magnets, he is also an outstanding expert in advising students. At the beginning of my study at MIT, he gave me very attentive instructions, which let me quickly adapt the environment. When I gradually got familiar with the study, his insights kept me always on the right track of research. He himself is a best example for me of being a first-class researcher.

The thesis can never be done without the selfless help from everybody in the lab. Thanks for Dr. Juan Bascuñán's generous sharing of his experience. He gave me many advices on my research and helped me out time after time. Thanks for Dr. Seungyong Hahn's unreserved sharing of his knowledge and ideas, which not only helped me do better in my research, but also greatly expanded my vision. The contents of the thesis were carefully revised by him. I would also like to thank Dr. John Voccio, with whom I am working tightly together on the MgB_2 project. Also, the language of this thesis was largely improved by his kindest help. I also want to thank Dr. Dongkeun Park and Dr. Youngjae Kim. We did many tests together, even late into night. I can hardly imagine how I could finish the tests without their help. I still need to thank David Johnson and Peter Allen, who helped me a lot in making the apparatus for the experiments.

Finally, I want to thank my wife, Wenqing Lu. She took a good care of me, so that I could thoroughly focus on the completion of the thesis.

This work was supported by the National Institute of Biomedical Imaging and Bioengineering for Research Resources.

Contents

1 Introduction **17**

1.1 Discovery of Superconductivity 17

1.2 Three Critical Parameters of Superconductors 18

1.3 Discovery of Various Superconductors 18

1.4 A Newly-discovered Superconductor, MgB_2, and Its Properties 21

1.5 MRI Magnets 22

1.5.1 Two Issues with MRI Magnets 23

1.5.2 MgB_2 vs. NbTi 25

1.5.3 Persistent-current Mode and Superconducting Joints 26

1.5.4 Challenges with Monofilament MgB_2 Wire: Flux Jumping . . 29

1.6 Overview 31

1.6.1 Research Goal 31

1.6.2 Research Plan 31

2 Short Sample Magnetization Tests **33**

2.1 Experimental Setup 33

2.1.1 Search Coil System 34

2.1.2 NbTi Background Magnet 38

2.1.3 Sample Holder Assembly 39

2.1.4 Liquid Helium 40

2.1.5 Power Supply 41

2.1.6 Data Acquisition System 41

2.2 Experimental Procedures 42

2.2.1 Sample Preparation 42
2.2.2 Test Procedures 45
2.3 Results and Disscussions 48
2.3.1 Magnetization Trace of Monofilament MgB_2 Wire 48
2.3.2 Magnetization Trace of Monofilament NbTi Wire 50

3 100-m Coil Tests **53**
3.1 Experimental Setup 53
3.1.1 Sample Container Assembly 53
3.1.2 JASTEC Magnet 59
3.1.3 Power Supplies 59
3.1.4 Data Acquisition System 60
3.2 Experimental Design 61
3.2.1 Design of Coils 61
3.2.2 Design of Current Lead Connectors 62
3.2.3 Purposes of the Tests 62
3.2.4 Test Plans 64
3.3 Experimental Procedures 65
3.3.1 Coil Preparation 65
3.3.2 Test Operations 66
3.4 Results and Discussions 68
3.4.1 Critical Current Comparison Between Multifilament and Monofilament MgB_2 Coils 68
3.4.2 Quench Safety at Critical Current 71
3.4.3 Kaiser Effect: No Mechanical Disturbance 72
3.4.4 Partial Flux Jumping 73
3.4.5 Premature Quench 79
3.4.6 Flux Jumping in Monofilament NbTi Coil 79

4 Conclusions **83**

List of Figures

1-1 Resistance vs. temperature curve of a few selected metals [1]. Horizontal axis is temperature in [K], vertical axis is electric resistance normalized to the resistance at zero Centigrade. The resistance of mercury drops to zero steeply at around 4.2 K. 18

1-2 A 3-D sketch of critical surface of superconductors. The vertical axis is current density. The horizontal axis is magnetic field. The outward axis is temperature. 19

1-3 The discoveries of various superconductors [2, 3]. The horizontal axis is the discovered year of each superconductor. The vertical axis is the critical temperature of each superconductor. The picture of J. Akimitsu was provided by Juan Bascuñán. 20

1-4 Comparison between two images obtained by different level MRI magnets [4]. The left image was obtained by a 7 T MRI magnet, the right image was obtained by a 1.5 T MRI magnet. The left image is clearer than the right one. 23

1-5 Normal mode and Persistent-current mode [5]. A magnet operated in normal mode is always driven by an external power supply. A magnet operated in persistent-current mode is first charged by an external power supply, and then disconnected from it. Current flows in the superconducting loop has negligible decay. 26

1-6 Cross section view of a multifilament MgB_2 wire and a monofilament MgB_2 wire [6]. Monofilament MgB_2 wire has a large and continuous cross section of MgB_2. 28

1-7 The critical currents of a typical monofilament MgB_2 joint. It is over 300 A at 15 K, self-field. "Test1" and "Test2" represent the first measurement and the second measurement of the same sample, respectively. 28

2-1 Schematic drawing of the bridge circuit of the search coil system [7]. A primary search coil, a secondary coil, and a balancing potentiometer are the key components in the circuit. 34

2-2 Search coils were wound on a Φ5/32-inch stainless steel tube. The primary search coil was wound at the center; the two split secondary coils were wound at two sides, 8.4 mm away from the center. The coils were wrapped by 3M yellow tapes. 37

2-3 The background magnet wound with AWG # 28 NbTi wire. The magnet could provide up to 3 T magnetic field at its center, at 4.2 K. 38

2-4 A schematic drawing of the samples, the background magnet and the search coils. Outermost is the background magnet. Samples are in the bore of the primary search coil. It is not to-scale. 39

2-5 The sample holder assembly. The left hand side is the top part of the sample holder; the right hand side is a complete view of the sample holder. 39

2-6 The power supply used to charge the NbTi background magnet. It is an Oxford model IPS 125-9 power supply. 41

2-7 The temperature profile of the heat treatment of the monofilament MgB_2 wire. The steps were: 30 minutes rise from room temperature to 500 C, 30 minutes held at 500 C, 30 minutes rise from 500 C to 700 C, and 90 minutes held at 700 C. Then the samples were cooled down to room temperature. 43

2-8 The short samples of monofilament MgB_2 and NbTi. The silver pile is MgB_2, the red pile is NbTi. 44

2-9 The installation of the short samples. Short samples of wires were fixed by two brass pieces at the center of the primary coil. The tube on which search coils were wound was fixed by the same brass pieces in the bore of the background magnet. 45

2-10 The sample holder was being inserted into the liquid helium dewar. . 46

2-11 Magnetization vs. field trace of short samples of monofilament MgB_2 wire. The horizontal axis is background magnetic field in [T]. The vertical axis is magnetization of the samples in [emu/cm^3]. 48

2-12 Magnetization vs. field traces of multifilament MgB_2 wire [8]. The horizontal axis is background magnetic field in [T]. The vertical axis is magnetization in [emu/cm^3]. The three traces are measured at 10 K, 20 K , and 30 K respectively. 49

2-13 Magnetization vs. field trace of short samples of monofilament NbTi wire. The horizontal axis is background magnetic field in [T], and the vertical axis is magnetization of NbTi in [emu/cm^3]. 51

3-1 The schematic drawing of the sample container assembly. The assembly is fitted in a stainless steel cryostat. 54

3-2 The sample container assembly in its rack. 55

3-3 Flange seen from the top. Goddard fittings and stainless steel tubes were fixed by epoxy to the flange. 56

3-4 Assembled aluminum chamber. 57

3-5 The copper can and the coil before they were assembled. 58

3-6 Aluminum chamber parts, styrofoam, and the copper can. They were placed in the order as they would be assembled. 58

3-7 The JASTEC magnet used in the 100-m coil tests. It can generate up to 5 T magnetic field at its center. The picture was taken when the cryostat and the sample container assembly was amounted in the bore. 59

3-8 HP power supplies used to charge the sample coils. 60

3-9 The assembled connectors through the hole of the aluminum chamber. 63

3-10 A wound 100-m MgB_2 coil before heat treatment. A few turns of stainless steel wire was wrapped to tighten the winding. The leads of the coil were tied on a stainless steel rod to avoid bending during heat treatment. 66
3-11 The winding machine used to wind all the 100-m sample coils. 67
3-12 Liquid helium transfer. On the top, liquid helium was being transferred from the liquid helium dewar to the cryostat through a transfer line. On the bottom, a high pressure helium column was giving pressure to the liquid helium dewar. 69
3-13 Critical currents of the 100-m multifilament MgB_2 coil, from 4.2 K to 15 K, in 1 T background field and self-field. 70
3-14 Critical currents of the 100-m monofilament MgB_2 coil, from 4.2 K to 15 K, in 1 T background field and self-field. 70
3-15 A voltage vs. current graph of monofilament MgB_2 coil. The horizontal axis is the transport current in [A]. The vertical axis is the voltage across the coil in [V]. The steep increase of the voltage indicates a quench at critical current. The coil survived from such quenches for multiple times. 71
3-16 Voltage vs. current curves of charging the monofilament MgB_2 coil up to different currents in sequence. Charging current started from low to high. None of the curves started with a quiet section. 73
3-17 The voltage vs. current curve when the monofilament MgB_2 coil was charged at 1 A/s. The coil quenched at critical current. 74
3-18 The voltage vs. current curve when the monofilament MgB_2 coil was charged at 2 A/s. The coil was discharged at 5 A/s. 75
3-19 The voltage vs. current curve when the monofilament MgB_2 coil was charged at 5 A/s. The coil was discharged at 5 A/s. 75
3-20 Current and voltage vs. time curves. The horizontal axis is the test time in [s]. The left vertical axis is the current flowing in the coil in [A]. The right vertical axis is the voltage across the coil in [V]. 77

3-21 Zoomed-in current and voltage vs. time curves. Where the voltage has a spike, the varying rate of current is slower. 77
3-22 The curve of differentiated current timing the inductance of the coil. It is in the unit of [V]. 78
3-23 Voltage vs. current curves of energizing the monofilament NbTi coil at 0.5 A/s and 1 A/s. Spikes were deep and almost down to 0. 80

List of Tables

1.1 Critical current densities of a few selected superconductors [7]. All the current densities are in [A/mm^2]. The "$\|$" following YBCO or Bi2223 means the field is applied parallel to the tape. The "$\perp$" means the field is applied perpendicular to the tape. 22

1.2 Comparison between NbTi and MgB_2 MRI magnets in critical temperature, operation temperature, major cooling mode, and operation mode. The critical temperatures here are of wires in self-field. 25

3.1 Geometric and electric properties of the 100-m coils. 62

Chapter 1

Introduction

1.1 Discovery of Superconductivity

In 1908, a Dutch scientist, Heike Kamerlingh Onnes, successfully liquified helium; it had been the last unliquified gas in the world. At that time, people already had the knowledge that electric resistance of pure metal drops when the temperature decreases. When helium was liquified, it provided the lowest temperature people could achieve at that time: 4.2 K. Onnes used his liquid helium to cool down various metals and tried to find out the relation between electric resistance and temperature. In 1911, when Onnes cooled mercury—the purest metal he could ever obtain—by liquid helium, he found surprisingly that the resistance of mercury steeply dropped to zero at about 4.2 K. The resistance vs. temperature curve is shown in Figure 1-1 [1].

The sharp transition clearly distinguishes mercury from other metals. Later, this characteristic of transition in resistance was given a name—"superconductivity", representing the superior ability of transporting electricity. However, the first-discovered superconductor, mercury, failed people in some way: it lost superconductivity even when it carried a tiny current. Apparently, besides temperature, superconductors have other critical parameters.

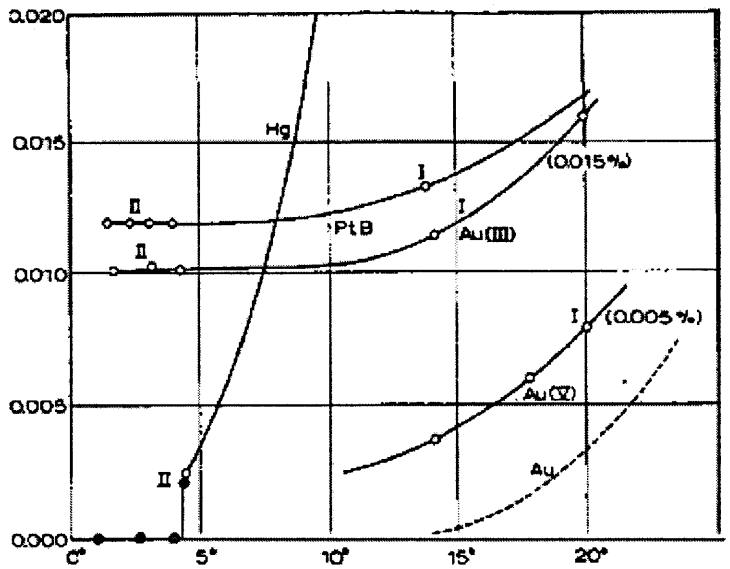

Figure 1-1: Resistance vs. temperature curve of a few selected metals [1]. Horizontal axis is temperature in [K], vertical axis is electric resistance normalized to the resistance at zero Centigrade. The resistance of mercury drops to zero steeply at around 4.2 K.

1.2 Three Critical Parameters of Superconductors

Figure 1-2 shows a 3-D curved surface. The three axes are current density (usually in [A/m^2]); temperature (usually in [K]) and magnetic field (usually in [T]). A superconductor is in superconducting state if all the three parameters are below this critical surface; otherwise it is in normal resistive state. The three parameters are all critical to the status of a superconductor. For safety, in real applications of superconducting devices, these parameters are usually designed below the critical values.

1.3 Discovery of Various Superconductors

Right after the superconductivity of mercury was discovered, a few other pure metals were discovered to be superconductors. Unfortunately, people found none of them would be able to carry a usable current. All these pure metals lost their superconductivities when a tiny current was applied.

The dream of making use of superconductors in real applications was delayed by

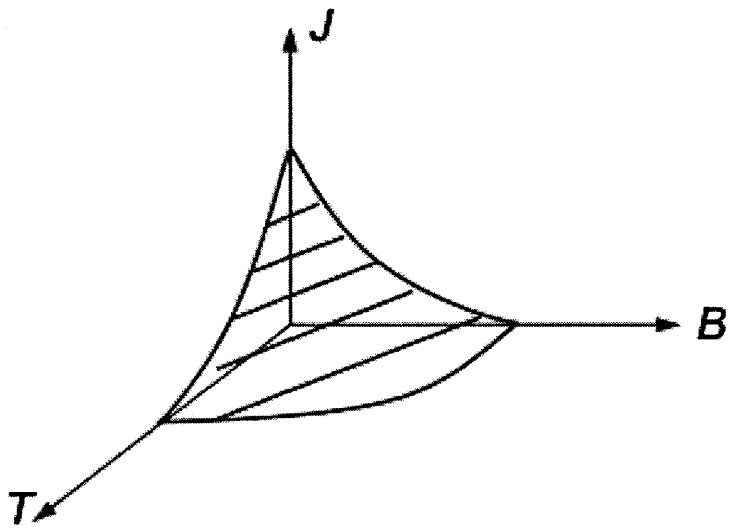

Figure 1-2: A 3-D sketch of critical surface of superconductors. The vertical axis is current density. The horizontal axis is magnetic field. The outward axis is temperature.

that problem for 50 years. In the late 1950s and early 1960s, two compounds were discovered to be superconductors—NbTi and Nb_3Sn [9]. These two compounds have well usable superconductivity: they can carry high current densities in high magnetic field. For example, both NbTi and Nb_3Sn have critical current densities higher than 2000 A/mm^2 in 5 T magnetic field. NbTi and Nb_3Sn enabled superconducting magnets to become a practical realization. Superconducting technologies associated with Nb-based superconductors were soon developed.

The two superconductors are the first two among those which are used in real applications. Their drawback is that the critical temperatures of both materials are very low. The critical temperatures of NbTi and Nb_3Sn are 9.8 K and 18.2 K respectively. It not only means that it is very costly to achieve their working condition, say, by cooling with liquid helium, but it also means that they are unstable when carrying high current, because the temperature margins are small. So, people still desired to discover new superconductors which have higher critical temperatures.

The breakthrough came in the mid-1980s when K. Müeller and J. Bednorz discovered a complex compound consisting of copper, oxygen and rare earth elements [10].

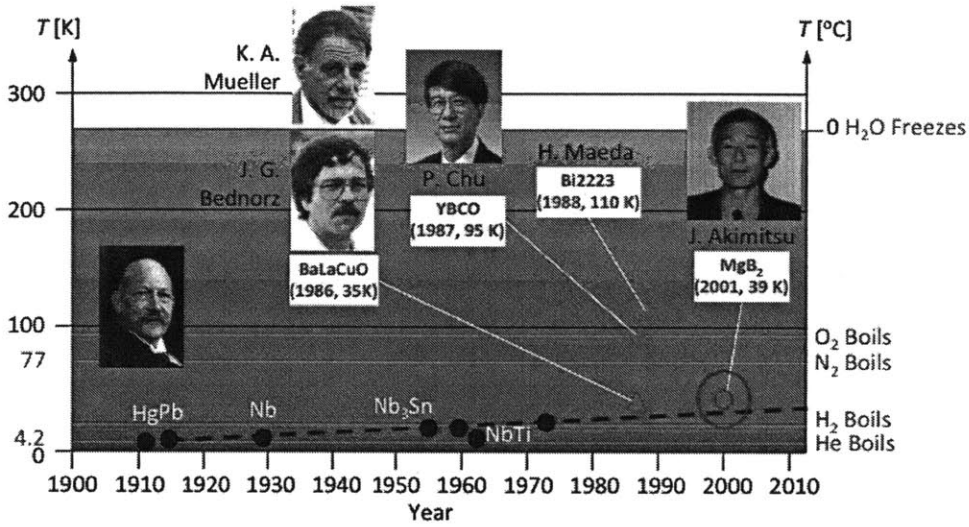

Figure 1-3: The discoveries of various superconductors [2,3]. The horizontal axis is the discovered year of each superconductor. The vertical axis is the critical temperature of each superconductor. The picture of J. Akimitsu was provided by Juan Bascuñán.

This discovery opened the gate to discovering high temperature superconductors. In the following few years, many compounds based on copper and oxygen were discovered to be superconductors, and the record of critical temperature was broken again and again. In the early 1990s, two compounds of this family, Bi2223 and YBCO [11, 12], were finally chosen to be commercially manufactured. They demonstrated high performance in magnetic field, and they are environmental friendly during production. Now, both Bi2223 and YBCO have well developed commercial products.

Figure 1-3 [2,3] summarizes the discoveries of various superconductors in a year vs. critical temperature graph. It shows a clear trend of discovering higher temperature superconductors.

1.4 A Newly-discovered Superconductor, MgB_2, and Its Properties

In 2001, a new superconductor—MgB_2—was discovered by J. Akimitsu [13]. It is an amazing discovery, because the components of the new superconductor are so simple. It consists of only two very common elements: magnesium and boron. While all the other high temperature superconductors contain rare earth elements which determine their high price, MgB_2 has a dominate price advantage against its rivals. In addition, the simple composition of MgB_2 makes its manufacturing easier and cheaper. The cost of MgB_2 wires is significantly lower than those of Bi2223 and YBCO. While the unit price is at least about \$20/m for Bi2223 tapes and \$40/m for YBCO tapes, the unit price for MgB_2 is only about \$2/m [14].

The critical temperature of MgB_2 is 39 K. Although this temperature is lower than the critical temperatures of Bi2223 and YBCO, it is significantly higher than those of NbTi and Nb_3Sn. This temperature, 39 K, is high enough to enable MgB_2 superconducting devices to be cooled by a moderate cryogenic cooler, instead of liquid helium or a very powerful cryogenic cooler. Making use of a cryogenic cooler could save liquid helium and thus cooling cost, which is a trend of superconducting technology.

Beside that the critical temperature and cost of MgB_2 are competitive, the critical current density of MgB_2 is also good in certain conditions. Table 1.1 lists the critical current densities of a few selected superconductors [7]. At 15 K, in a magnetic field of 3 T, MgB_2 has a critical current density of 1160 A/mm^2, which is larger than YBCO and Bi2223 in the some condition. Although NbTi and Nb_3Sn have larger critical current densities as 2000 A/mm^2, those have to be at 4.2 K. So, in liquid-helium-free and low-field applications, MgB_2 is no doubt an exceptional choice.

T [K]	Superconductor	3 T	5 T	8 T
4.2	NbTi	>3000	2500	1000
	Nb_3Sn	>2000	>2000	>2000
	MgB_2	1930	900	165
	YBCO‖	1350	1270	1155
	⊥	425	310	230
	Bi2223‖	900	900	900
	⊥	560	530	500
15	MgB_2	1160	280	20
20	MgB_2	585	80	Not Superconducting
	YBCO⊥	130	90	65
	Bi2223‖	730	650	575
	⊥	385	325	260

Table 1.1: Critical current densities of a few selected superconductors [7]. All the current densities are in [A/mm^2]. The "‖" following YBCO or Bi2223 means the field is applied parallel to the tape. The "⊥" means the field is applied perpendicular to the tape.

1.5 MRI Magnets

Magnetic resonance imaging (MRI) is a medical imaging technique used in radiology to visualize internal structures of the body in detail. MRI makes use of the property of nuclear magnetic resonance to image nuclei of atoms inside the body [15].

An MRI unit is a device in which the patient or a part of the patient, like a limb, lies. An important part of an MRI unit is a large, homogenous magnet. The magnet generates a strong and uniform magnetic field which causes certain spinning nuclei in the body, usually hydrogen nuclei, or protons, to radiate. The radiation is captured and recorded by a scanner, and an image of the scanned object is constructed. Since each water molecule contains two hydrogen nuclei and the distribution of water in the body varies in different tissues, the distribution of hydrogen nuclei can be used to distinguish different tissues in human body.

Obviously, the stronger the magnetic field is, the higher frequency radiation the hydrogen nuclei generate. So, a gradient magnetic field will cause hydrogen nuclei in different position radiate at different frequency. The difference in frequency can then be used to find the origin of the radiation. In this way, a higher magnetic field can make stronger contrast between different tissues. Therefore, higher magnetic field

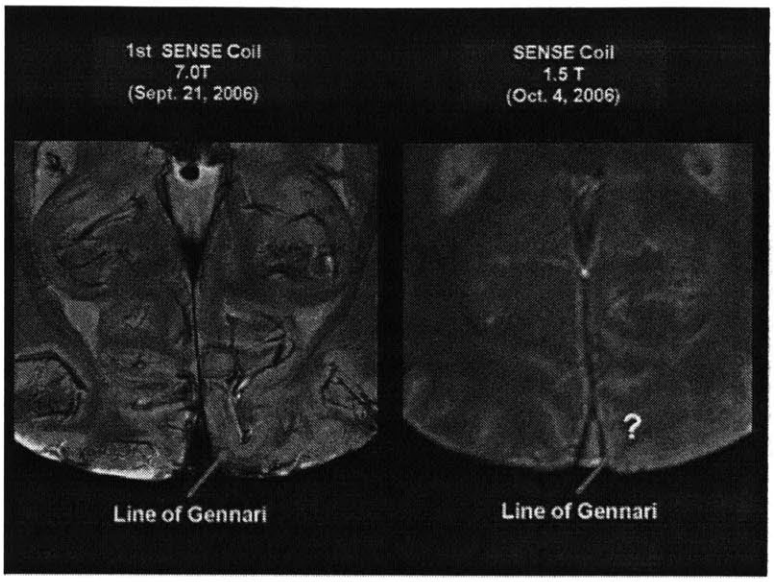

Figure 1-4: Comparison between two images obtained by different level MRI magnets [4]. The left image was obtained by a 7 T MRI magnet, the right image was obtained by a 1.5 T MRI magnet. The left image is clearer than the right one.

produces higher resolution images. Figure 1-4 [4] shows a comparison between two images obtained in fields. The left image was obtained by a 7 T MRI magnet, while the right image was obtained by a 1.5 T MRI magnet. We can clearly see that the left image shows many details that are vague in the right one.

Since traditional electromagnets are made of copper, the magnetic field is limited by the power and cooling capacity of the magnets. It is very difficult for a copper magnet to generate a magnetic field above 1 T in a large bore in which a human can lie. But now large MRI magnets are enabled by superconducting technology. Nowadays, well over 20,000 MRI magnets are installed in hospitals worldwide, and the number is still increasing by 10% annually [16].

1.5.1 Two Issues with MRI Magnets

At present, most of the commercial superconducting MRI magnets are made of NbTi or Nb_3Sn, due to their good electrical and mechanical properties. However, these MRI magnets have two issues—(1) premature quench and (2) liquid helium consumption, which makes the manufacturing and operating of an MRI magnet expensive.

Premature Quench

The first issue associated with NbTi or Nb_3Sn MRI magnets is premature quench. It has been a long time since people first met with this issue, but there is still not a good method that can solve it thoroughly. NbTi or Nb_3Sn magnets are usually working in liquid helium at 4.2 K, leaving a temperature margin of only 0.5~2 K in self-field [17]. They could be turned into normal state by a thermal disturbance. When a zone of NbTi becomes resistive in the winding, there is still high current flowing in the wire. So, it will release a large amount of Joule heat in the normal state zone. This normal zone could propagate rapidly, turning the entire magnet into normal state. This leads to a final failure of the magnet. Because this event could happen when the applied current is below the critical current, it is called a premature quench.

People now are able to eliminate most of the sources of disturbances from the magnets. For example, people have developed multifilament wires to avoid flux jumping, and people "train" the magnets to eliminate mechanical disturbances. However, not all disturbances can be thoroughly removed, and some finished magnets still have premature quench [18, 19]. Those magnets cannot be sold which drags down the producibility of the magnets and hence increases the manufacturing cost.

Liquid Helium Consumption

The second issue associated with NbTi or Nb_3Sn MRI magnets comes from liquid helium. Helium is a non-renewable resource, so it is expensive, and its price keeps rising. Making the situation worse, most helium mines are located in North America, and helium is limited exporting to other countries. So, the price of liquid helium outside U.S. is even higher [3]. This makes it very expensive to operate an MRI magnet in Asia or in Africa, where residents earn little and cannot afford an MRI examination.

	NbTi	MgB_2
Critical Temperature	9.2 K	39 K
Operating Temperature	4.2 K	10~15 K
Major Cooling Mode	Liquid Helium	Cryo-cooler
Operating Mode	Persistent-current mode	Persistent-current mode

Table 1.2: Comparison between NbTi and MgB_2 MRI magnets in critical temperature, operation temperature, major cooling mode, and operation mode. The critical temperatures here are of wires in self-field.

1.5.2 MgB_2 vs. NbTi

MRI magnets are critical for quality health care. They are very useful in early detection and efficient treatment of disease or injury. However, the over 20,000 MRI units benefit only about 10% of the total humanity, chiefly in the developed nations, because NbTi MRI magnets are very expensive not only in manufacturing but also in operating [20]. Our goal is to develop low-cost, easy-to-operate MRI units which serve to the rest 90% of the humanity.

We choose MgB_2 superconducting wires as a way approaching that goal. Compared with NbTi, MgB_2 has a few features which could make building an MRI magnet cheaper. Table 1.2 lists a few comparison between MRI magnets made of the two superconductors. The critical temperature of NbTi is 9.2 K, while it is 39 K for MgB_2. NbTi magnets are usually cooled by liquid helium and work at 4.2 K, costing a lot to operate. Also, the temperature margin of NbTi and Nb_3Sn (0.5~2 K) is small, which makes the magnets unstable. The critical temperature of MgB_2 is 39 K, allowing MgB_2 magnets to be cooled by moderate cryogenic coolers. This could reduce a lot of operation cost. In addition, the temperature margin could be bigger than 2 K; MgB_2 magnets are supposed to work more stable than NbTi magnets.

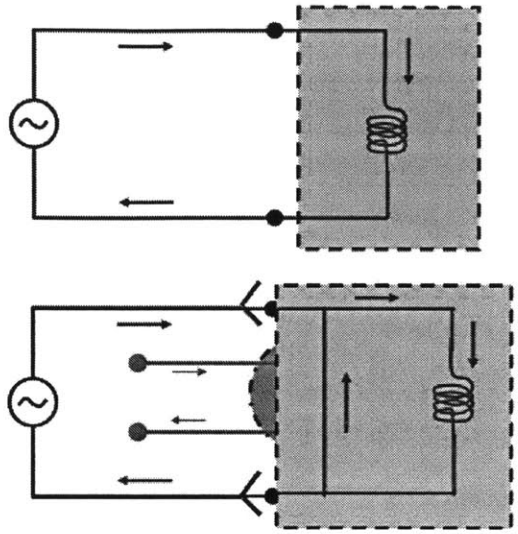

Figure 1-5: Normal mode and Persistent-current mode [5]. A magnet operated in normal mode is always driven by an external power supply. A magnet operated in persistent-current mode is first charged by an external power supply, and then disconnected from it. Current flows in the superconducting loop has negligible decay.

1.5.3 Persistent-current Mode and Superconducting Joints

Persistent-current Mode and Normal Mode

Before we can start to build MgB_2 MRI magnets, we have a few technical issues to solve. Because power supplies usually fluctuate intolerably compared with the requirement of an MRI signal, so in order to keep the current flowing in an MRI magnet constant, in most cases, the magnet is operated in persistent-current mode.

In persistent-current mode, once an MRI magnet is charged, it will be disconnected from the power supply and the current flows in a superconducting loop with negligible decay. This operation mode makes use of superconductivity of the magnets. A schematic drawing of persistent-current mode operation is shown in Figure 1-5 [5]. In contrary, in normal mode, a magnet is always connected to a power supply, and the current flowing in the magnet is solely supplied by the power supply. Since a power supply fluctuates, the magnetic field generated by the magnet also fluctuates, which fails to meet the ppm field-homogeneity requirement of an MRI magnet.

In persistent-current mode, the entire magnet system consists of three essential

parts: the magnet itself, a persistent-current switch, and a superconducting joint. When the magnet is being charged, the switch is turned on and has a large resistance. Little current flows through it. Once the magnet is charged to the desired level, the switch is turned off and becomes superconducting. Then the current flowing in the magnet passes the superconducting joint. The power supply can be disconnected at this time. Now, the entire loop is superconducting, and the current in the loop stays extremely constant.

Superconducting Joints

In a persistent-current mode magnet, a superconducting joint plays a critical role. In order to have a constant current in the coil loop, the total resistance of the loop should be zero. So, the joint connecting the two ends of the coil should be superconducting and be able to carry a large enough current.

The technique of fabricating superconducting NbTi joints has been well developed for NbTi MRI magnets. For MgB_2 MRI magnets, we tried to make superconducting joints with multifilament MgB_2 wire [21]. Unfortunately, the technique of multifilament MgB_2 superconducting joints is not reliable; the producibility of the joints is not high enough for mass production.

Recently, we have made a reliable success in making superconducting joints with monofilament MgB_2 wire. Compared with multifilament MgB_2 wire, monofilament wire has a large and continuous cross section of MgB_2 (see Figure 1-6 [6]), which ensures a good connection between the MgB_2 core in the wire and the MgB_2 block in the joint holder. Currently, we can make good superconducting MgB_2 joints with monofilament wire, having high critical currents. The critical current of joints is over 300 A at 15 K, in self-field. The critical current measurement of a typical joint is shown in Figure 1-7.

Since we can make reliable superconducting MgB_2 joints only with monofilament MgB_2 wire, in order to enable persistent-current mode MgB_2 MRI magnets, we have to choose monofilament MgB_2 wire as the conductor.

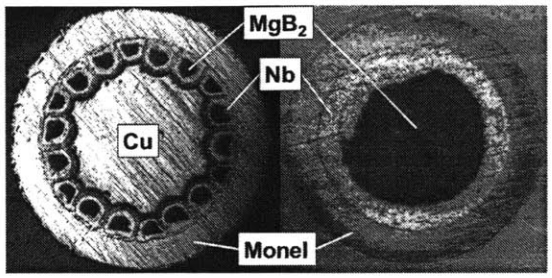

Figure 1-6: Cross section view of a multifilament MgB_2 wire and a monofilament MgB_2 wire [6]. Monofilament MgB_2 wire has a large and continuous cross section of MgB_2.

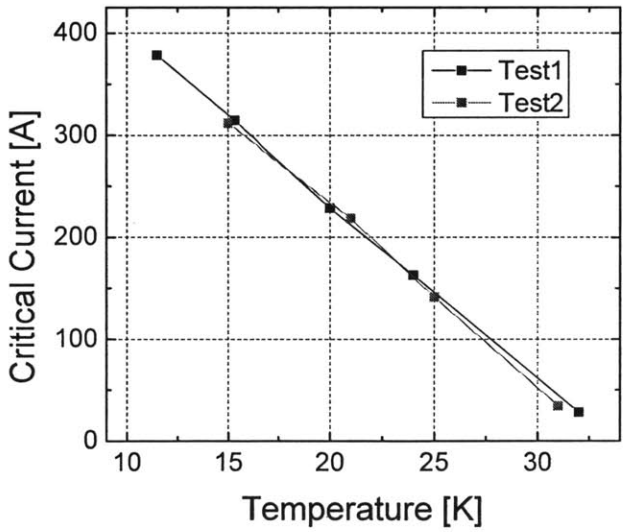

Figure 1-7: The critical currents of a typical monofilament MgB_2 joint. It is over 300 A at 15 K, self-field. "Test1" and "Test2" represent the first measurement and the second measurement of the same sample, respectively.

1.5.4 Challenges with Monofilament MgB_2 Wire: Flux Jumping

In early 1960s, right after people discovered Nb_3Sn and NbTi, superconductors were made in the form of monofilament wires. People soon found that magnets wound with monofilament wires were impossible to reach the expected critical currents; they quenched at much lower currents. Later, a phenomenon called "flux jumping" was discovered to be the major cause of the failures of these magnets.

When a block of superconductor is in a magnetic field, its magnetization state is not stable. A thermal disturbance could come from mechanical movement or electromagnetic change. For example, the movement of a length of wire in the winding or the growth of a crack in the epoxy releases a heat disturbance. Or, a changing current generates heat in superconductors due to AC loss. The thermal disturbance raises the temperature slightly in the superconductor. Due to the temperature rise, the critical current density decreases. Because of the redistribution of the screening current, the change of critical current density causes a flux motion in the superconductor, which further releases energy and heats up the superconductor. In the case when the released energy is high enough, it will cause an avalanche of releasing energy and flux motion. This process is flux jumping [22]. If the process ends when the external magnetic field partially penetrates into the superconductor, it is a partial flux jumping. If the external magnetic field penetrates the entire superconductor, it is a full flux jumping. In extreme cases, a flux jumping would turn a superconductor to normal. If flux jumping happens in a superconducting magnet, the magnet could have premature quenches.

The criterion for flux jumping is developed in thermodynamics. People compared the energy released by a flux movement and the enthalpy of a superconductor, by the following criteria [7]:

$$\frac{\mu_0 J_c^2 a^2}{3\rho C(T_c - T_o)} < 1 \tag{1.1}$$

and

$$\frac{\mu_0 J_c^2 a^2}{3[H(T_c) - H(T_o)]} < 1 \tag{1.2}$$

In Inequality 1.1, μ_0 is permeability in free space, J_c is critical current density, a is the half depth of the superconductor or radius of a filament, ρ is the density of the superconductor, C is the specific heat of the superconductor, T_c is the critical temperature, and T_o is the operating temperature. In Inequality 1.2, $H(T_c)$ and $H(T_o)$ is the enthalpy of the superconductor at critical temperature and working temperature respectively.

Inequality 1.1 determines whether or not a flux jumping would be initiated, but it does not tell if the flux jumping would process completely; Inequality 1.2 determines whether or not a full flux jumping would happen. From the criteria, we can see that a small a value or a large $T_c - T_o$ value prevents the happening of flux jumping. This means a big gap between critical temperature and working temperature, or a small filament size is preferred to avoid flux jumping. While the critical temperature is fixed with a certain superconductor, this conclusion initiated people to develop multifilament superconductors. Now, most of the commercial NbTi and Nb_3Sn wires are multifilament.

Since MgB_2 has a higher critical temperature, it is possible that MgB_2 can have a larger filament size while not having flux jumping. Substituting property values of MgB_2 into Inequality 1.1 and assuming an MgB_2 magnet is working at 15 K, the critical filament size determined by Inequality 1.1 is 1.3 mm. This value is close to the wire we want to use. Therefore, theoretically, monofilament MgB_2 wire could be free of flux jumping, and experiments are required to further investigate the flux jumping characteristic. In contrast, if a NbTi magnet is working at 4.2 K, the critical filament size is only about 100 μm.

1.6 Overview

1.6.1 Research Goal

The aim of the thesis is to prove that we can employ monofilament MgB_2 wire to build MRI magnets yet not having flux jumping issue. If monofilament MgB_2 wire does the job, then we can make use of our reliable superconducting MgB_2 joint technique. With superconducting MgB_2 joints, we are able to build persistent-current mode MgB_2 MRI magnets. The proof of no flux jumping in monofilament MgB_2 wire is the key to persistent-current mode MgB_2 MRI magnets.

1.6.2 Research Plan

From the flux jumping criteria, we have already known that monofilament MgB_2 wire thinner than 1.3 mm may not have flux jumping. In order to demonstrate this with experiments, we designed a series of tests:

a) Magnetization tests of short samples to show monofilament MgB_2 wire does not have flux jumping.

b) Comprehensive tests of 100-m sample coils wound with multifilament MgB_2, monofilament MgB_2 and monofilament NbTi to show monofilament MgB_2 coil does not have premature quench.

If the results of the two sets of tests are positive, they together guarantee that monofilament MgB_2 magnets will not have any unwanted effect of flux jumping.

Short Sample Tests

The tests of short samples consist of two parts:

a) Measurement of magnetization trace of short samples of monofilament MgB_2 wire.

b) Measurement of magnetization trace of short samples of monofilament NbTi wire.

Short samples of monofilament NbTi wire are tested as a control group. They are supposed to have flux jumping in contrast with MgB_2.

100-m Coil Tests

Once we demonstrate that short samples of monofilament MgB_2 wire does not have flux jumping, we start the 100-m coil test. The tests of 100-m coils consist of the tests of three coils:

a) Test of a 100-m coil wound with multifilament MgB_2 wire.

b) Test of a 100-m coil wound with monofilament MgB_2 wire.

c) Test of a 100-m coil wound with monofilament NbTi wire.

Multifilament MgB_2 coil and monofilament NbTi coil are tested as control samples. A monofilament MgB_2 coil is supposed to perform as well as a multifilament MgB_2 coil in terms of critical current and stability; a monofilament NbTi coil is supposed to have flux jumping and premature quench.

Chapter 2

Short Sample Magnetization Tests

The purpose of short sample magnetization tests are to find out whether or not there is flux jumping in monofilament MgB_2 wire, before we do coil tests, by measuring the magnetization trace of short samples of monofilament MgB_2 wire. Magnetization trace has been widely used to examine NbTi and Nb_3Sn and other superconductors. Magnetization trace tells much information about the superconductor regarding critical current, critical field, and flux jumping issue. In the thesis, our analysis focuses on flux jumping issue only.

2.1 Experimental Setup

In order to measure the magnetization traces of the short samples of superconductors, an inclusive experimental setup was required: 1) a search coil system that captured the magnetic signals; 2) a sample holder assembly that held the samples and other affiliated parts; 3) a NbTi background magnet that provided a background magnetic field up to 3 T; 4) liquid helium that cooled the samples and other parts down to 4.2 K; 5) a power supply that supplied current to the background magnet; 6) and a data acquisition system that collected and recorded all the signals during the experiments.

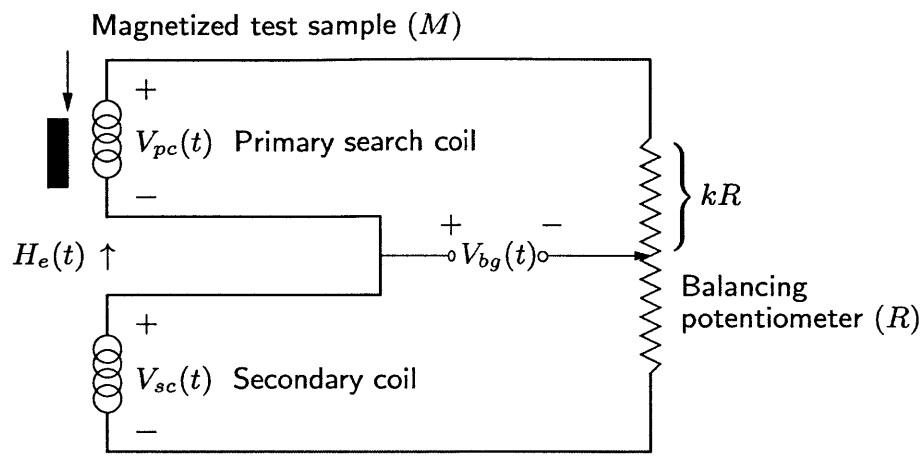

Figure 2-1: Schematic drawing of the bridge circuit of the search coil system [7]. A primary search coil, a secondary coil, and a balancing potentiometer are the key components in the circuit.

2.1.1 Search Coil System

Principle of Search Coil System

Search coils are widely used to measure magnetization traces. Figure 2-1 [7] shows a schematic drawing of the electric circuit of the search coils system. The core component of the system consists of: 1) a primary search coil surrounding the samples; 2) a secondary coil with an empty bore (or in some cases the secondary search coil is split into two or more coils); 3) a balancing potentiometer. They are connected in a bridge circuit. To measure the magnetization trace of samples, a steadily varying magnetic field is applied evenly in the space. While the samples are magnetized by the magnetic field, the primary search coil captures the total magnetic flux change within its bore, including both the background field and the magnetization of the samples. The secondary coil or coils at the same time collect solely the change of the background field. The background field components from both coils then cancel each other in the bridge circuit. A balancing potentiometer is used to make the cancellation complete.

When a uniform time-varying magnetic field $H_e(t)$ is applied in the space, the voltages induced by $H_e(t)$ across the primary search coil V_{pc} and secondary coil V_{pc}

are [7]:

$$V_{\mathrm{pc}}(t) = \mu_0 N_{\mathrm{pc}} A_{\mathrm{pc}} \left[\frac{dM}{dt} + \left(\frac{d\tilde{H}_{\mathrm{e}}}{dt} \right)_{\mathrm{pc}} \right] \tag{2.1a}$$

$$V_{\mathrm{sc}}(t) = \mu_0 N_{\mathrm{sc}} A_{\mathrm{sc}} \left(\frac{d\tilde{H}_{\mathrm{e}}}{dt} \right)_{\mathrm{sc}} \tag{2.1b}$$

The subscripts pc and sc refer to primary search coil and secondary coil respectively. μ_0 is the permeability in free space. N is the number of turns of each coil. A is the average effective area of turns in the coil through which $H_{\mathrm{e}}(t)$ occupies. M is the magnetization of the samples. $\tilde{H}_{\mathrm{e}}$ is the space-averaged field of $H_{\mathrm{e}}(t)$ over each coil.

Then the output voltage $V_{\mathrm{bg}}(t)$ across the bridge can be obtained by [7]:

$$V_{\mathrm{bg}}(t) = (k-1)V_{\mathrm{pc}}(t) + kV_{\mathrm{sc}}(t) \tag{2.2}$$

In this equation, k is a constant (range from 0 to 1) representing the fraction of resistance on the primary search coil side. By combining Equation 2.1 and Equation 2.2, we can get [7]:

$$\begin{aligned} V_{\mathrm{bg}}(t) =& (k-1)\mu_0 N_{\mathrm{pc}} A_{\mathrm{pc}} \frac{dM}{dt} \\ &+ (k-1)\mu_0 N_{\mathrm{pc}} A_{\mathrm{pc}} \left(\frac{d\tilde{H}_{\mathrm{e}}}{dt} \right)_{\mathrm{pc}} + k\mu_0 N_{\mathrm{sc}} A_{\mathrm{sc}} \left(\frac{d\tilde{H}_{\mathrm{e}}}{dt} \right)_{\mathrm{sc}} \end{aligned} \tag{2.3}$$

If we appropriately adjust the value of k and make $\frac{d\tilde{H}_{\mathrm{e}}}{dt}$ terms cancel each other completely, namely,

$$(k-1)\mu_0 N_{\mathrm{pc}} A_{\mathrm{pc}} \left(\frac{d\tilde{H}_{\mathrm{e}}}{dt} \right)_{\mathrm{pc}} + k\mu_0 N_{\mathrm{sc}} A_{\mathrm{sc}} \left(\frac{d\tilde{H}_{\mathrm{e}}}{dt} \right)_{\mathrm{sc}} = 0 \tag{2.4}$$

and then

$$V_{\mathrm{bg}}(t) = (k-1)\mu_0 N_{\mathrm{pc}} A_{\mathrm{pc}} \frac{dM}{dt} \tag{2.5}$$

In this condition the output voltage $V_{\mathrm{bg}}(t)$ is solely a function of M. In practice, the background field term cannot cancel each other completely, but Equation 2.5 still holds very well. In most cases, the value of k is close to 0.5 if the search coils are designed properly.

If we integrate both sides of Equation 2.5, we can find that the magnetization of the sample is proportional to the integration:

$$\int_0^t V_{\mathrm{bg}}(\tau)d\tau = (k-1)\mu_0 N_{\mathrm{pc}} A_{\mathrm{pc}} M(H_{\mathrm{e}}) \tag{2.6a}$$

$$M(H_{\mathrm{e}}) = \frac{\int_0^t V_{\mathrm{bg}}(\tau)d\tau}{(k-1)\mu_0 N_{\mathrm{pc}} A_{\mathrm{pc}}} \tag{2.6b}$$

Once we measure and record V_{bg}, we can obtain the magnetization of the samples by using Equation 2.6.

The background field is supposed to be uniform in space theoretically. However, in some cases, when the background field is generated by a small magnet, it is not perfectly uniform even in the space occupied by the samples. In these cases, the samples and the primary search coil should be placed at the center of the background magnet where the field is most uniform. The secondary coil then should be split into two coils and placed at both sides of the primary coil. They are kept at a constant distance; so, if the coils are not perfectly placed, one coil would collect more flux while the other would collect less. The sum of the flux they collect will not change too much; so, the coils are position insensitive. The two secondary coils are connected in series, and V_{sc} is now the voltage across both of them.

Winding of Search Coils

Figure 2-2 shows the search coils used in the tests. Three coils were wound: one primary search coil, and two split secondary coils. In this experiment, the background magnetic field was generated by a small NbTi magnet; the field was not uniform in

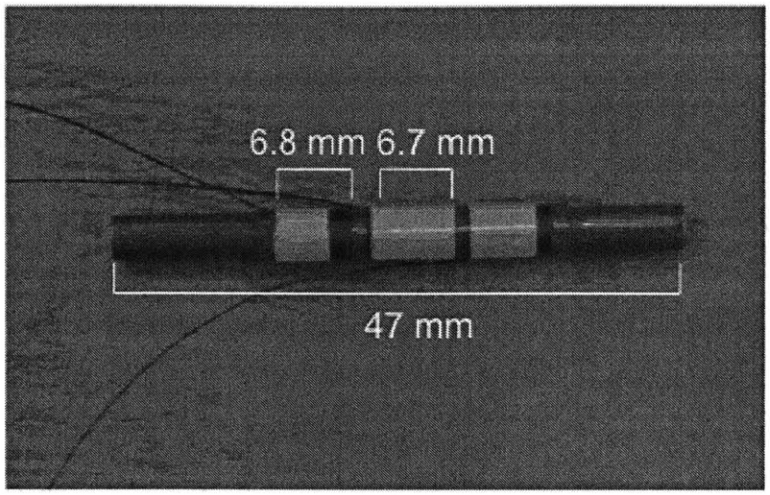

Figure 2-2: Search coils were wound on a Φ5/32-inch stainless steel tube. The primary search coil was wound at the center; the two split secondary coils were wound at two sides, 8.4 mm away from the center. The coils were wrapped by 3M yellow tapes.

the space where measurements took place. So the primary search coil was placed at the center of the field, so that the samples would be in the most uniform field. The secondary coil was split into two coils and wound on two sides of the primary coil. Because the background field was symmetric, this winding could make use of the symmetry and get more stable signals. In order to make k close to 0.5, the secondary coils were designed longer than they would be in a uniform field. In the end, the primary search coil was 6.7 mm long and each of the secondary coils was 6.8 mm long.

All the search coils were wound with AWG # 38 copper wires on a Φ5/32-inch stainless steel tube. The center of the secondary coils was 8.4 mm away from the center of the primary coil. Scotch tape was wrapped around the tube to separate the coils and fix them in position. The primary coil had 100 turns and the secondary coils had 101 turns each. They were wound in two layers. All the coils were wound manually. When the winding finished, 3M yellow tape was wrapped around the coils to prevent them from loosening. The leads of the coils were left long and they extended from the low temperature zone to room temperature area. The coils were connected outside the liquid helium dewar with a potentiometer to form a bridge circuit.

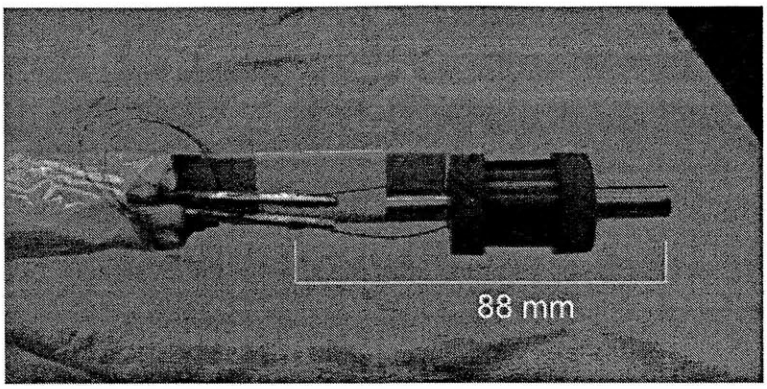

Figure 2-3: The background magnet wound with AWG # 28 NbTi wire. The magnet could provide up to 3 T magnetic field at its center, at 4.2 K.

Balancing Potentiometer

The total resistance of the potentiometer is 100 Ω. The potentiometer had to be properly adjusted before the bridge circuit could output correct signals. Otherwise, Equation 2.4 would not hold, and there would be some $V_{\mathrm{bg}}(t)$ in Equation 2.5 even when there were no M. An inclined curve would be obtained in this situation.

To adjust the potentiometer, we did the magnetization test without any sample. We kept doing the tests while changing the partition of the potentiometer, until the obtained magnetization trace was almost flat. Then we knew that the potentiometer was properly adjusted; we kept it unchanged during the entire tests. The ratio of partition of the potentiometer, namely, the value of k in Equation 2.2, turned out to be 5.47 for this experimental setup.

2.1.2 NbTi Background Magnet

Figure 2-3 shows the background magnet. It was wound on a Φ1/4-inch stainless steel tube with AWG # 28 NbTi wire. It could provide up to 3 T magnetic field at its center when 60 A current was passing its winding. In order to have the most uniform field, the center of the primary search coil coincided with the center of the background magnet. The relative positions of the search coils, the background magnet, and the samples are shown in Figure 2-4.

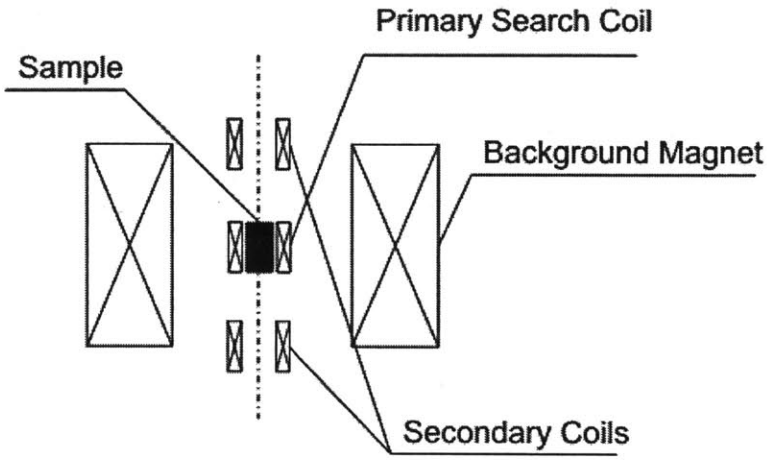

Figure 2-4: A schematic drawing of the samples, the background magnet and the search coils. Outermost is the background magnet. Samples are in the bore of the primary search coil. It is not to-scale.

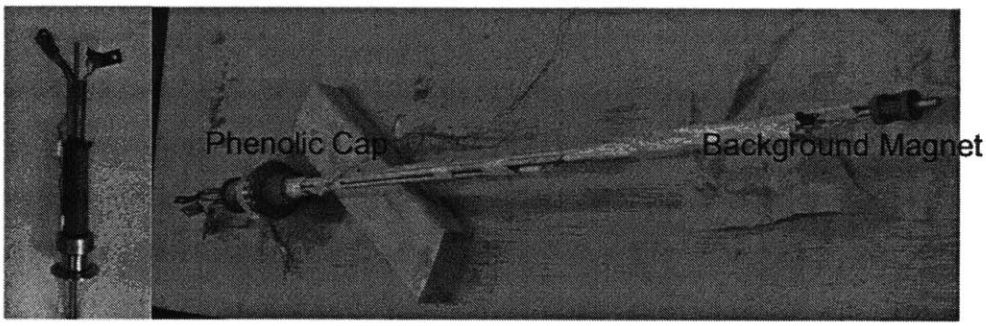

Figure 2-5: The sample holder assembly. The left hand side is the top part of the sample holder; the right hand side is a complete view of the sample holder.

2.1.3 Sample Holder Assembly

A complete sample holder assembly included the following parts: a center supporting tube, two tubes for current leads, a tube for signal wires, and other affiliated parts.The top sections of these tubes were surrounded by a phenolic tube and they were fixed into a phenolic plate which covered the phenolic tube. All the fittings between the stainless steel tubes and phenolic pieces were fixed and sealed by Stycast 2850 epoxy. A stainless steel Goddard fitting was used to connect the phenolic part of sample holder to the neck of a liquid helium dewar. Figure 2-5 is a picture of the sample holder assembly with zoomed-in top part on the left.

The center Φ1/4-inch stainless steel tube played the role as the support of the entire assembly. The top end of the tube was sealed by rubber, and the bottom end was attached to the background magnet, search coils and samples. The current leads were made of a pair of AWG # 12 copper wires and they were inserted in a pair of Φ1/8-inch stainless steel tubes. They conducted current to the background magnet. Both of the copper wires were stripped in order to have a good contact with helium vapor. While the Goddard fitting sealed the dewar, helium vapor vented through the tubes and cooled the current leads efficiently. Signal wires were made of AWG # 32 copper wire, and all pairs of wires were twisted in order to avoid noise.

2.1.4 Liquid Helium

Liquid helium was used in the tests to provide a cryogenic environment for the samples. Because the NbTi background magnet had to work at 4.2 K, the background magnet, the search coils and the samples were immersed in liquid helium during the entire tests.

In the tests, liquid helium was supplied by the MIT Cryolab. It was delivered in a 60 L liquid helium dewar. Our sample holder was designed to fit the neck of the dewar. A Goddard fitting was used for the connection; the bottom of the fitting was attached to a stainless steel flange which fitted the flange on the neck of the dewar. When doing tests, the sample holder together with the samples was inserted into the dewar and then fixed and sealed by the pair of flanges.

The Goddard fitting could move along the phenolic tube; thus, when the Goddard fitting was fixed to the neck of the dewar, the sample holder could move upward or downward to adjust the position of the samples. The best position for the NbTi background magnet and the samples was just below the level of liquid helium. In this way the heat conduction through the sample holder could be reduced to minimum; while the NbTi magnet and the samples were still safely cooled by liquid helium.

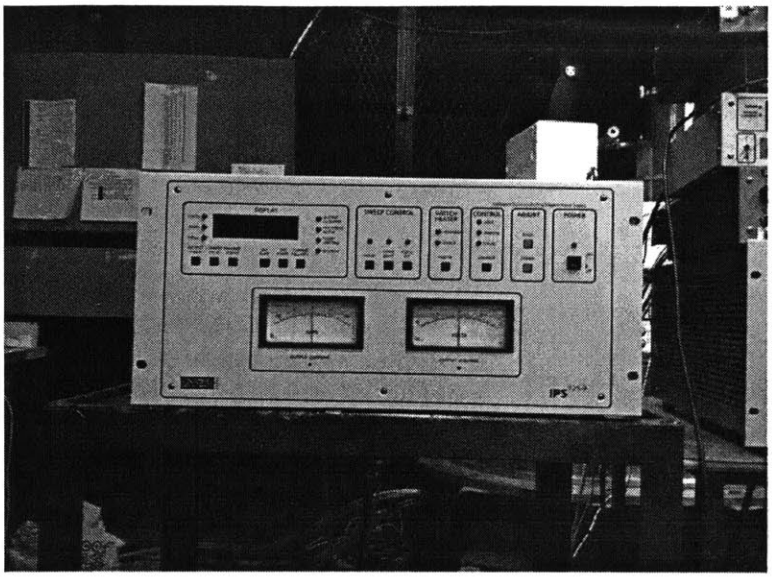

Figure 2-6: The power supply used to charge the NbTi background magnet. It is an Oxford model IPS 125-9 power supply.

2.1.5 Power Supply

In all the tests, an Oxford model IPS 125-9 power supply was employed to supply current to the background magnet. The power supply is shown in Figure 2-6. The power supply can provide up to ±125 A current, with voltage compliance from −9 V to +9 V and ramping rate from 0.01 A/min up to 1200 A/min. The output current is stable, fluctuating within ±3 mA range, as long as the ambient temperature is constant (within ±1 C). This power supply is perfect for charging a NbTi magnet.

2.1.6 Data Acquisition System

In the tests, voltage signals were collected and recorded by SCXI data acquisition system, and finally stored in a desktop computer. The voltage signals included:

- Current flowing in the background magnet. The current flew through a shunt across which a shunt voltage could be measured. The voltage was proportional to the current flowing in the shunt. From the value of current, we could calculate the field generated by the background magnet.

- Bridge voltage of the search coils circuit. The voltage was later integrated and the integration is proportional to the magnetization of the samples.

The temperature was measured by a Cernox™ sensor. The signal generated by the Cernox™ censor was sent to Cryocon 14 temperature monitor and displayed in absolute temperature there. The Cernox™ sensor was mounted right above the NbTi background magnet and the samples. During the tests, the readout of the measured temperature should be kept at 4.2 K. Then we were sure that the NbTi magnet and the samples were in the liquid helium.

2.2 Experimental Procedures

2.2.1 Sample Preparation

Preparation of Short Samples of Monofilament MgB_2 Wire

The MgB_2 wire was manufactured by Hyper Tech Research, Inc. The wire was delivered in a 300-m spool. The diameter of the wire is 0.84 mm bare. The wire consisted of a MgB_2 core in a niobium tube. The cross section area of the MgB_2 core was 25% of cross section area of the entire wire. Outside the niobium was a layer of copper. The cross section area of copper was 0.16 mm^2. When 100 A current were carried in the wire, and MgB_2 core suddenly lost its superconductivity, the copper layer could carry a current no more than 625 A/mm^2. A layer of monel (an alloy of nickel and copper) was at outermost of the wire. When delivered, the wire was insulated by S-glass sleeve. In the magnetization tests, we removed the S-glass layer in order to get a higher superconducting to non-superconducting ratio in volume.

The MgB_2 wire was unreacted when it was delivered. The MgB_2 core consisted of only magnesium and boron powder mixture in a preferred ratio. In order to make the wire have superconductivity, we needed to heat treated the wire in our furnace. Many tests had been done regarding the heat treatment parameters. The determined temperature profile of the heat treatment was: rise from room temperature to 500 C in 30 minutes, hold at 500 C for 30 minutes, rise from 500 C to 700 C in 30 minutes,

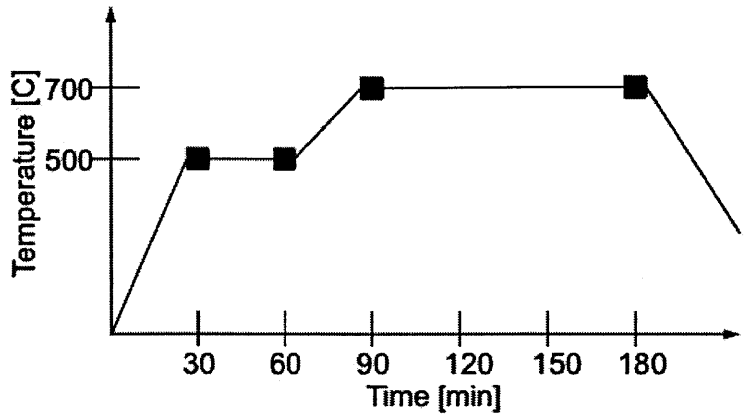

Figure 2-7: The temperature profile of the heat treatment of the monofilament MgB_2 wire. The steps were: 30 minutes rise from room temperature to 500 C, 30 minutes held at 500 C, 30 minutes rise from 500 C to 700 C, and 90 minutes held at 700 C. Then the samples were cooled down to room temperature.

and then hold at 700 C for 90 minutes. The heat treatment was protected in argon gas (1 atm at room temperature and ~3 atm at 700 C). After these steps finished, the heating stopped immediately. The samples were left in the furnace and cooled down until they reached the room temperature. This procedure had been proved to be a good heat treatment for monofilament MgB_2 wire by previous heat treatment experiments. A temperature profile of the heat treatment is shown in Figure 2-7.

During the heat treatment, the sample wire was in the form of a long piece. The two ends of it were sealed by ceramic, in order to prevent magnesium from evaporating. After the heat treatment finished and the sample wire cooled down to room temperature, the wire was cut into 6.8 mm long short pieces, which was the length of the primary search coil. The two cut ends of the short samples were sanded to flat. Some short samples of monofilament MgB_2 are shown in Figure 2-8. The MgB_2 samples are the silver pile in the picture.

Short Samples of Monofilament NbTi Wire

The monofilament NbTi wire was manufactured by Supercon, Inc. The diameter of the wire is 0.8 mm. The NbTi core took 25% of the cross section area. A layer of copper was outside the NbTi filament. There was no insulation material outside the

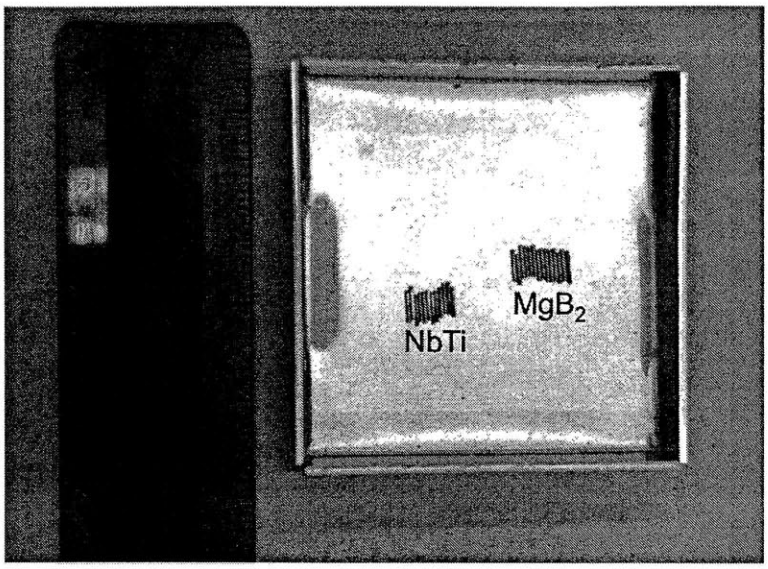

Figure 2-8: The short samples of monofilament MgB_2 and NbTi. The silver pile is MgB_2, the red pile is NbTi.

copper.

To prepare the short samples for the tests, the NbTi wire was cut into 6.8 mm short pieces. As with the MgB_2 short samples, both ends of the samples were sanded to flat for a better installation. Some short samples of NbTi are shown in Figure 2-8. The NbTi samples are the red pile in the picture.

Samples Installation

The short samples of wires were installed inside the tube on which search coils were wound. In order to fill the entire space in the bore of the primary search coil, 12 short samples were inserted into the search coil and tested at the same time. Two brass pieces were machined to hold the two ends of the tube in order to fix the samples at the center of the primary search coil. The tube on which search coils were wound was fixed by the same brass pieces in the bore of the background magnet. The lengths of the brass pieces were delicately designed so as to make sure the center of the samples, the center of the primary search coil and the center of the background magnet were coincide. A picture of the assembly is shown in Figure 2-9. The assembly was then attached to the bottom end of the sample holder.

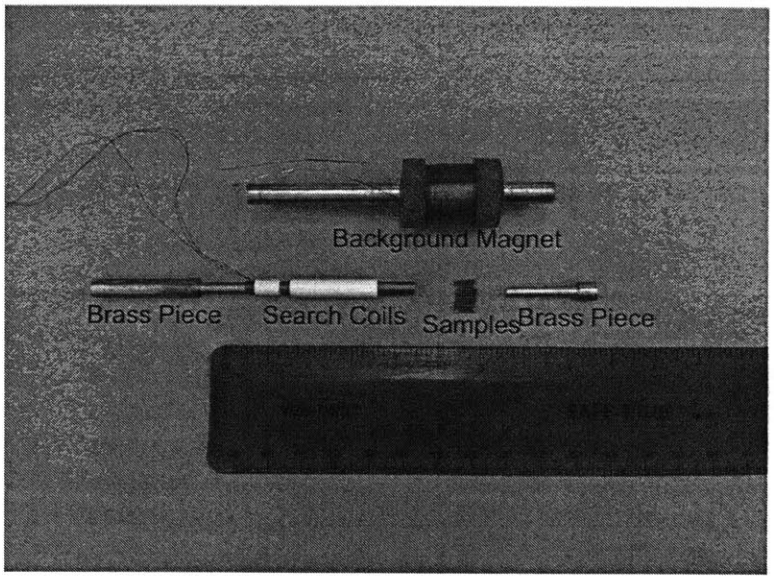

Figure 2-9: The installation of the short samples. Short samples of wires were fixed by two brass pieces at the center of the primary coil. The tube on which search coils were wound was fixed by the same brass pieces in the bore of the background magnet.

2.2.2 Test Procedures

After the samples were installed, they were ready to be tested in liquid helium. Before the sample holder went into liquid helium dewar, it was first cooled by liquid nitrogen. Liquid nitrogen is much cheaper than liquid helium and it has much larger specific heat, which makes it to be the best pre-cooling cryogen.

After the bottom part of the sample holder was pre-cooled by liquid nitrogen to 77 K, it was immediately inserted into the liquid helium dewar. The Goddard fitting on top of the sample holder fixed the holder and sealed the dewar. A Cernox™ temperature sensor was attached above the background magnet to make sure the magnet was immersed in liquid helium; otherwise, the position of the sample holder could be adjusted vertically. Figure 2-10 was taken when the sample holder was being inserted into the liquid helium dewar. After the sample holder was mounted, the signal wires were then connected to the data acquisition system. And the current leads for the background magnet were connected to the Oxford power supply.

Because the magnetization of superconductors depends on the history of how it is magnetized, it is very important to keep a "virgin" state of the samples before

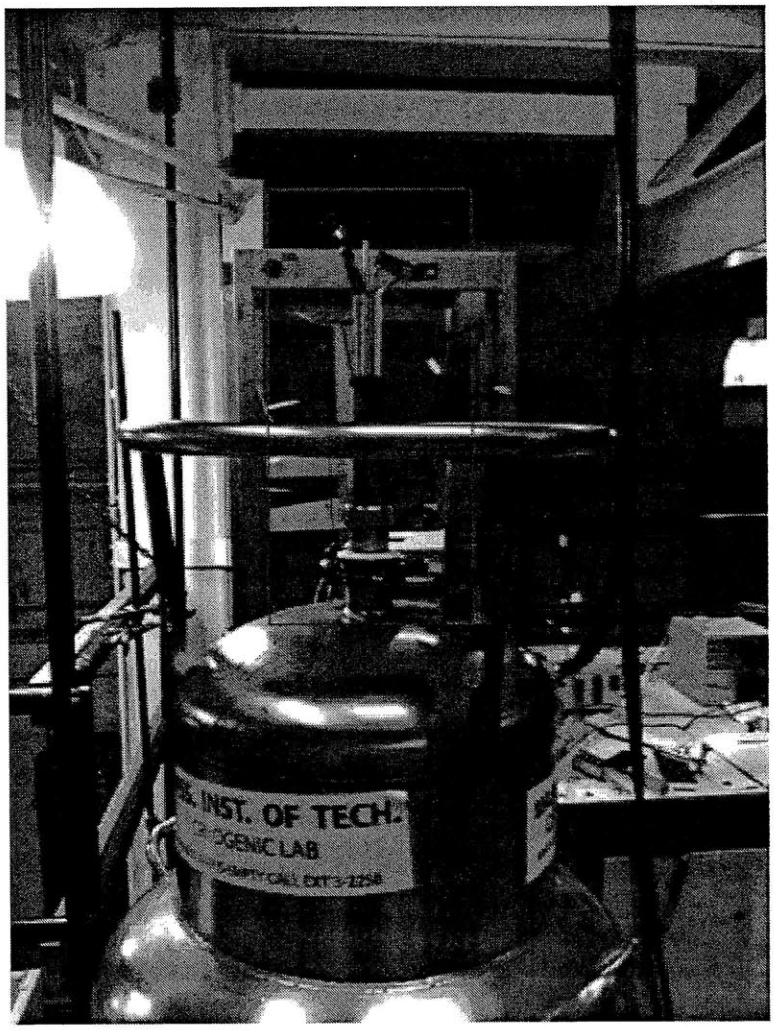

Figure 2-10: The sample holder was being inserted into the liquid helium dewar.

the tests can be started. In order to get a good magnetization trace, the samples should not have been magnetized. So every time we wanted to re-test the samples, we had to lift the samples above liquid helium, waited until the samples warmed up above 39 K. The samples lost superconductivity when they were warmed up. Then we cooled them by immersing them in liquid helium again. The samples became"virgin" superconductor and we could do the magnetization test again.

When all the wires were connected and the samples were at 4.2 K, we could start to charge the background magnet. The output current rose from 0 to 60 A with a ramping rate of 600 A/min. This means that the background magnet generated a magnetic field from 0 to 3 T at a sweeping rate of 0.5 T/s. After reaching the peak value, the current was kept at the peak for a few seconds in order to wait the field to be stable. Then the magnet ramped down passing zero point toward the opposite polarity. After waiting for another few seconds we ramped the magnet up back to its positive polarity, staying there for a few seconds and finally the magnet went back to 0.

The entire sweeping process was kept at a constant ramping rate of 0.5 T/s. From Equation 2.5 we know that the signal strength is proportional to the ramping rate of the background field. So a fast sweeping process helps us obtain clear magnetization traces. Also important is the number of turns of the search coils, and the area of the bore of the coils. We wound 100 turns as the primary search coil, and we tested 12 samples at the same time. All of these actions led to a strong enough bridge voltage which could be easily distinguished from noise.

During the sweeping process, we kept collecting and recording the magnitude of the applied current from which we could calculate the magnitude of the background field, also the bridge voltage which gave us the magnetization of the samples. Once we got the magnetization of the samples and the corresponding background field, we can draw them on a single 2-D graph. This was how we obtained the magnetization traces.

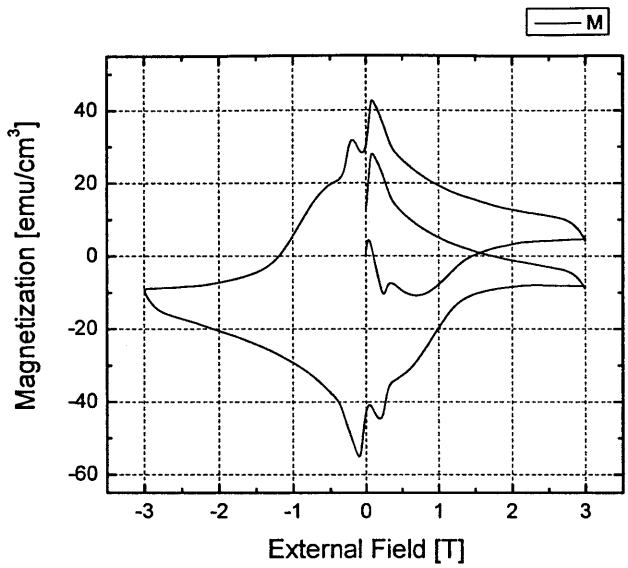

Figure 2-11: Magnetization vs. field trace of short samples of monofilament MgB_2 wire. The horizontal axis is background magnetic field in [T]. The vertical axis is magnetization of the samples in [emu/cm^3].

2.3 Results and Disscussions

2.3.1 Magnetization Trace of Monofilament MgB_2 Wire

The magnetization trace of short samples of monofilament MgB_2 wire is shown in Figure 2-11. The horizontal axis is background magnetic field in [T], and the vertical axis is magnetization of the samples in [emu/cm^3]. The unit of [emu/cm^3] is equal to 0.001257 [T] in SI unit system. The unit of [emu/cm^3] was used because we could have a directly comparison between 2-11 and 2-12. The test was carried out at 4.2 K. For comparison purposes, a typical magnetization trace of multifilament MgB_2 wire is shown in Figure 2-12 [8].

From Figure 2-11 we can see that the magnetization trace of monofilament MgB_2 is essentially smooth. If there were flux jumping, the trace would have many teeth, as the trace of monofilament NbTi wire. This means that monofilament MgB_2 wire essentially does not have flux jumping issue.

The original measured bridge voltages had a thermal drift. When there was no

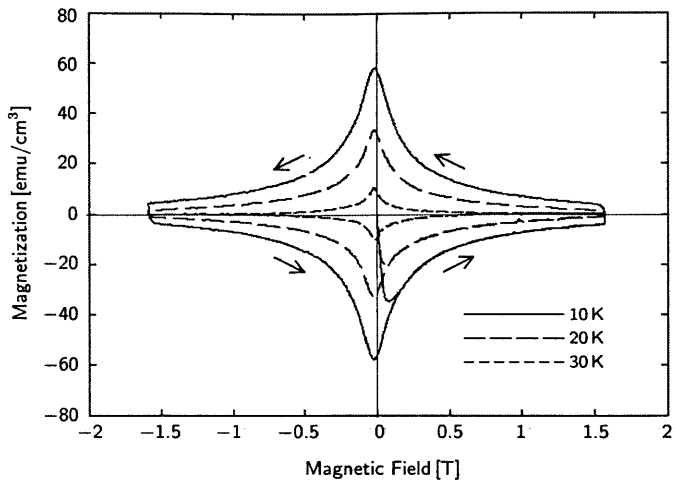

Figure 2-12: Magnetization vs. field traces of multifilament MgB_2 wire [8]. The horizontal axis is background magnetic field in [T]. The vertical axis is magnetization in [emu/cm^3]. The three traces are measured at 10 K, 20 K , and 30 K respectively.

background field, the bridge voltage should be zero theoretically. However, in the tests, because of the thermal drift, the bridge voltage was not zero even when the samples were "virgin". This drift had to be removed by subtracting a constant to the measured voltage before the voltage could be integrated. In addition, there was a signal drift of the data acquisition system too. During a full cycle of a measurement, the voltage signal could drift by 10^{-7} V, which was large enough to affect the final magnetization trace. In Figure 2-11, the second cycle of the trace does not overlap the first cycle very well. Also, the trace is not centered vertically. These distortions were due to the drifts in the tests.

An interesting phenomenon is that there are small dents at the peaks of the trace. The first dent occurred when the sample was fully magnetized for the first time. The other dents occurred when the background field was zero and the magnetization of the samples was maximum. All the dents occurred at a local peak on the trace where the background field was low, no more than 0.5 T. For superconductors, low external magnetic field allows high critical current density. According to Inequality 1.1, for the same samples, the other parameters are constant. The high J_c is more likely to make the left side of the inequality larger than 1. This explains why the dents occurred

where the background field is low and the magnetization is high.

A dent means there was a partial flux jumping happened. But the dent is small and does not go all the way down to zero, the flux jumping is also a partial one. If it happens in a magnet, it is very likely that the flux jumping is recoverable and does not cause a quench. Still, from the short sample magnetization tests, we cannot conclude whether or not monofilament MgB_2 wire is suitable for MRI magnets; we need to test monofilament MgB_2 wire in the form of a coil in order to draw further conclusion.

2.3.2 Magnetization Trace of Monofilament NbTi Wire

The magnetization test of monofilament NbTi wire was to make sure that the entire design and setup of the experiment was correct by showing that short samples of monofilament NbTi wire do have flux jumping. If the experiment is proved to be correct, the magnetization results of monofilament MgB_2 short samples are reliable.

The magnetization trace of short samples of monofilament NbTi wire is shown in Figure 2-13. The horizontal axis is background magnetic field in [T]. The vertical axis is magnetization of NbTi in [emu/cm^3]. The test was carried out at 4.2 K.

In Figure 2-13 we can clearly see flux jumping happened. Flux jumping happened when the samples were being magnetized. In addition, at the center of the trace, where the background field was zero and the critical current density was maximum, there are dents too. Unlike the case of monofilament MgB_2, the dents here are much deeper. Magnetization of the samples was supposed to be maximum at the center; while the flux jumping removed the peaks thoroughly.

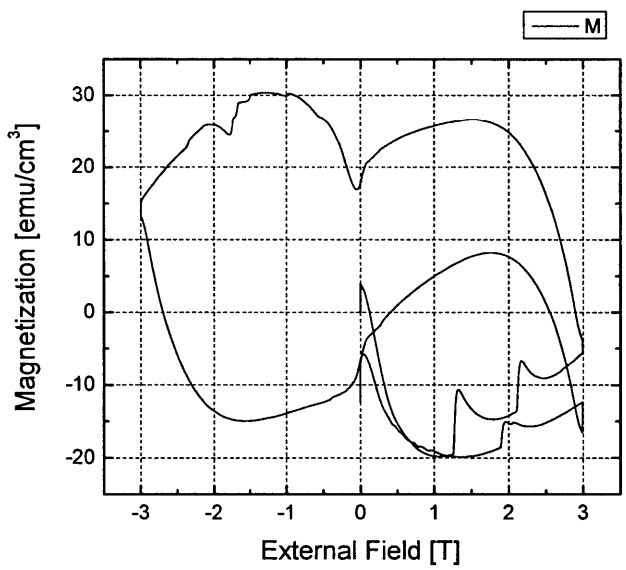

Figure 2-13: Magnetization vs. field trace of short samples of monofilament NbTi wire. The horizontal axis is background magnetic field in [T], and the vertical axis is magnetization of NbTi in [emu/cm^3].

Chapter 3

100-m Coil Tests

In the short sample tests, we have seen that monofilament MgB_2 wire only has minor flux jumping. In order to find out whether this flux jumping would cause a premature quench of a coil, we did a series of 100-m coil tests.

3.1 Experimental Setup

The 100-m coils were bigger than the short samples; also, we needed to control the temperature between 4.2 K and 15 K. The entire experimental setup was more complicated than short sample tests. In order to prepare the coil tests, we needed to design and make the sample container assembly and set up the data acquisition system. A background magnet and power supplies were also necessary.

3.1.1 Sample Container Assembly

In the 100-m coil tests, we needed to test the coils at a controlled temperature other than 4.2 K, and the temperature should be uniform in the entire coil. A sample container assembly was specially designed and made for testing 100-m coils at 4.2 K in background magnetic field. The sample container could provide an isothermal environment for the coils where the temperature ranged from 4.2 K to 15 K. The assembly was designed to fit in a stainless steel cryostat in which liquid helium was

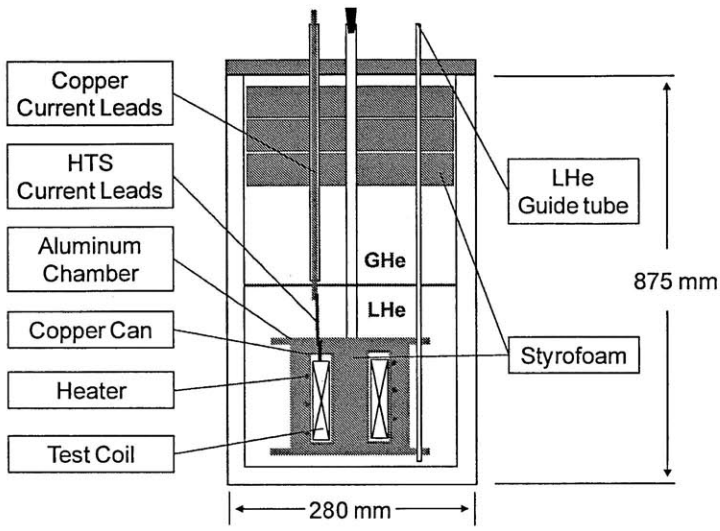

Figure 3-1: The schematic drawing of the sample container assembly. The assembly is fitted in a stainless steel cryostat.

filled; the cryostat was placed in the bore of the background magnet during the tests. A schematic drawing of the assembly is shown in Figure 3-1. The real assembly is shown in Figure 3-2.

Top Flange

The top part of the assembly included a flange, 6 layers of shields, a few functional stainless steel tubes going through them and a few functional holes left on the flange and in the shields.

The flange was made of G10. Two Φ5/16-inch stainless steel tubes were fixed on the flange, in which 7 bare AWG # 12 copper wires were bonded as the current leads for the 100-m coil. A Φ1/4-inch stainless steel tube was left for all the signal wires. All the tubes were fixed on the flange and sealed by Stycast 2850 epoxy. A Goddard fitting was mounted on the flange for the guide line of liquid helium. Two more Goddard fittings were mounted on the flange. They were used as vents when the liquid helium was being filled. Another Goddard fitting at the center of the flange was left for a Φ1/2-inch stainless steel tube which was the center supporting tube. This tube directly connected with the isothermal chamber. During the tests, the

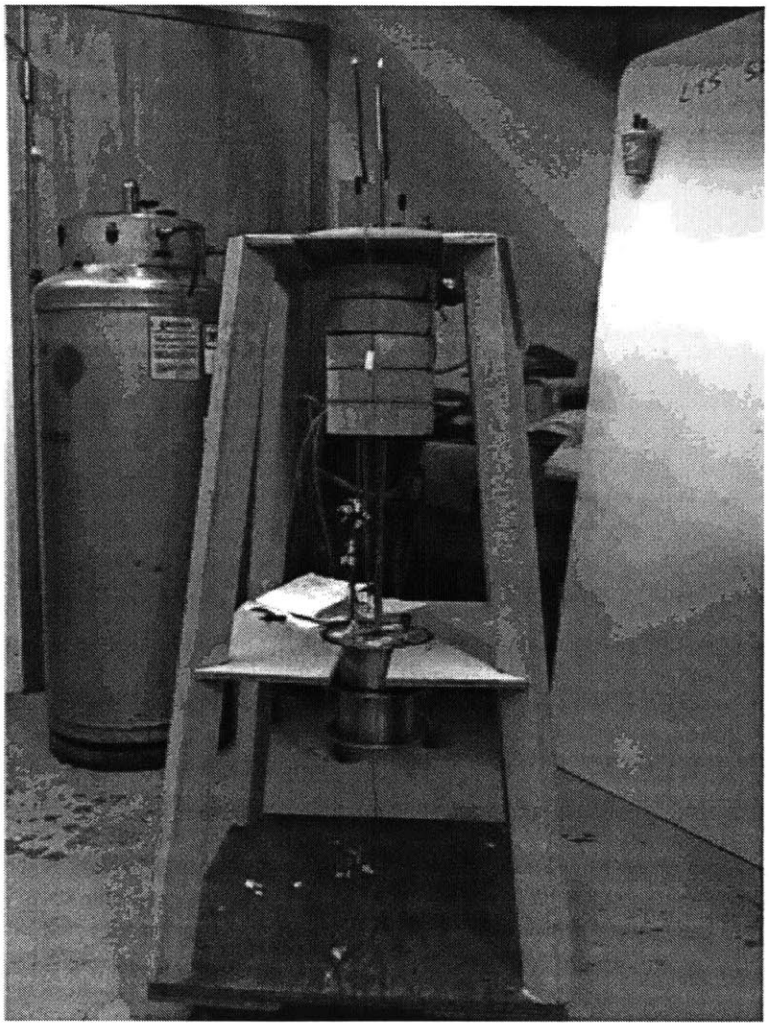

Figure 3-2: The sample container assembly in its rack.

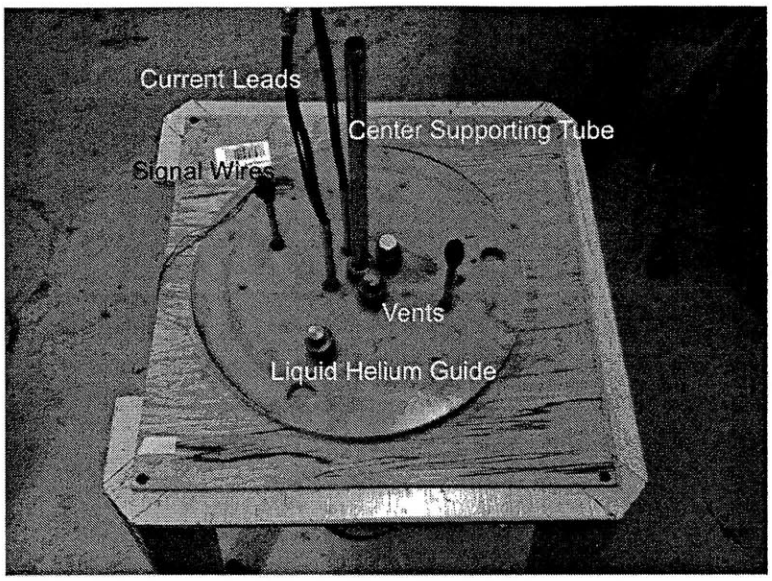

Figure 3-3: Flange seen from the top. Goddard fittings and stainless steel tubes were fixed by epoxy to the flange.

center tube, together with the isothermal chamber, was fixed by the Goddard fitting to the flange. A picture taken from the top of the flange is shown in Figure 3-3.

Shields were designed to reduce the heat transfer from the top. The shields consisted of 6 layers of styrofoam and copper plate composite. The copper plates were used to reduce the radiation. The styrofoam was used to reduce the conduction and convection in air. When the entire assembly was cooled by liquid helium, there would be a huge amount of evaporation of helium. So, a few holes were cut through the styrofoam and copper plates. Together with the holes left on the flange, they served as the vents for helium vapor.

Isothermal Chamber

Connected to the top flange with a center supporting tube was an isothermal chamber made of aluminum. The chamber had a cap and a bottom plate covering both ends of a Φ6-inch aluminum tube. At the top, middle and bottom of the chamber, there were side fins to catch the cooling from helium vapor. Figure 3-4 shows the chamber when it was assembled.

Inside the chamber, there was a small can made of copper designed to fit the

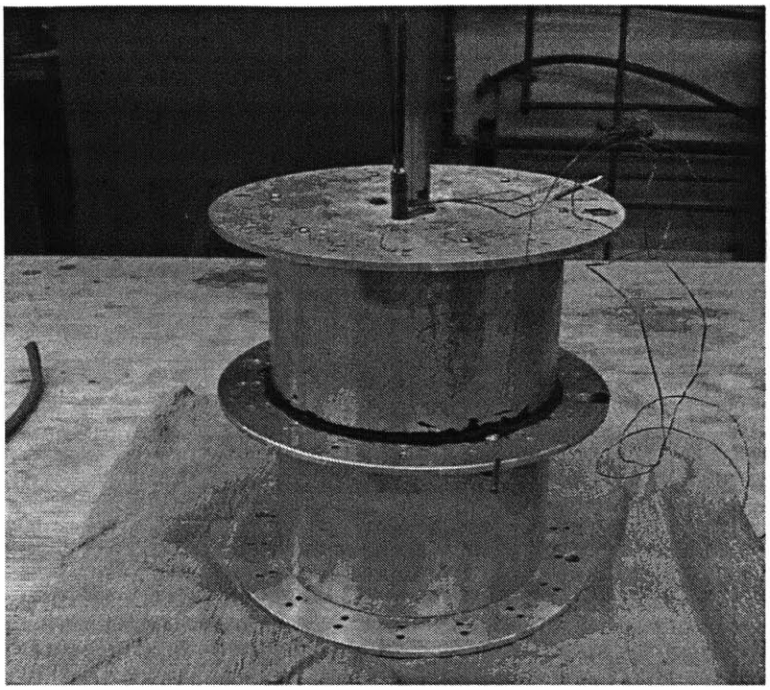

Figure 3-4: Assembled aluminum chamber.

100-m coils. The copper can consisted of a center tube, a wall tube, a top plate and a bottom plate. The center tube was used to fix the coils in place and enhance the heat conduction from the can to the coils. Thermal paint was employed to enhance the conduction between contacted surfaces. A piece of Chromel resistive wire was wound around the wall of the copper can serving as a heater. When the entire assembly was in liquid helium, the heater could heat up the copper can and keep an isothermal environment in it. Blocks of styrofoam were used to fill the vacancy inbetween the aluminum chamber and the copper can. They supported the copper can while allowing a minimal heat conduction. In addition, the styrofoam filled almost all the space in the aluminum chamber. So, not too much liquid helium was vaporized when the copper can was heated up. Figure 3-5 shows the copper can and the coil before they were assembled. Figure 3-6 shows how the copper can was assembled in the aluminum chamber.

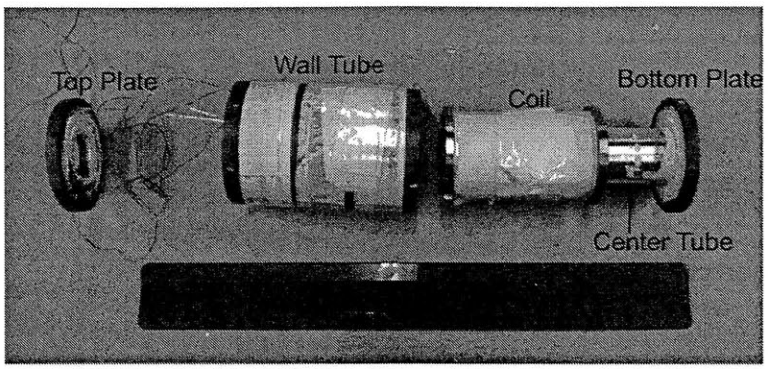

Figure 3-5: The copper can and the coil before they were assembled.

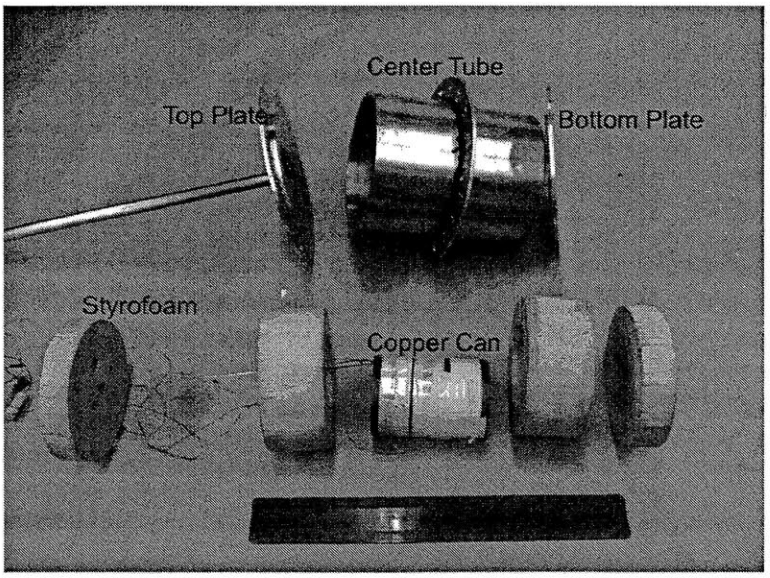

Figure 3-6: Aluminum chamber parts, styrofoam, and the copper can. They were placed in the order as they would be assembled.

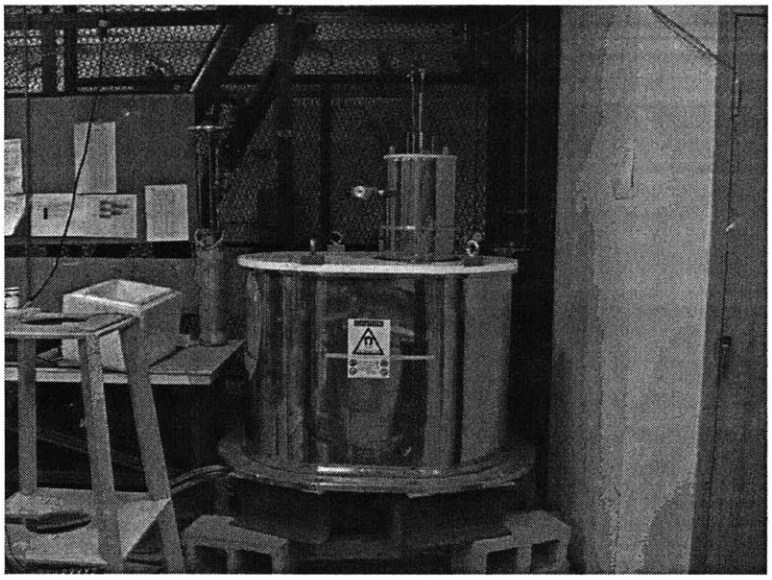

Figure 3-7: The JASTEC magnet used in the 100-m coil tests. It can generate up to 5 T magnetic field at its center. The picture was taken when the cryostat and the sample container assembly was amounted in the bore.

3.1.2 JASTEC Magnet

A dry NbTi magnet was used to provide the background magnetic field. The magnet was manufactured by JASTEC Co., Ltd. It can generate up to 5 T magnetic field in its 300 mm room temperature bore. When doing liquid helium experiment in high background field, we usually use a stainless steel cryostat as the container of liquid helium and place it in the bore of JASTEC magnet. The sample container assembly was inserted in the cryostat. The vertical position of the cryostat was adjusted so as to make sure the sample coil was at the center of the JASTEC magnet. The picture of JASTEC magnet is shown in Figure 3-7 when the cryostat and the sample container assembly was amounted in the bore.

3.1.3 Power Supplies

In the coil tests, two major power supplies were required. One power supply was used to charge the JASTEC magnet. The other power supply was used to charge the sample coils.

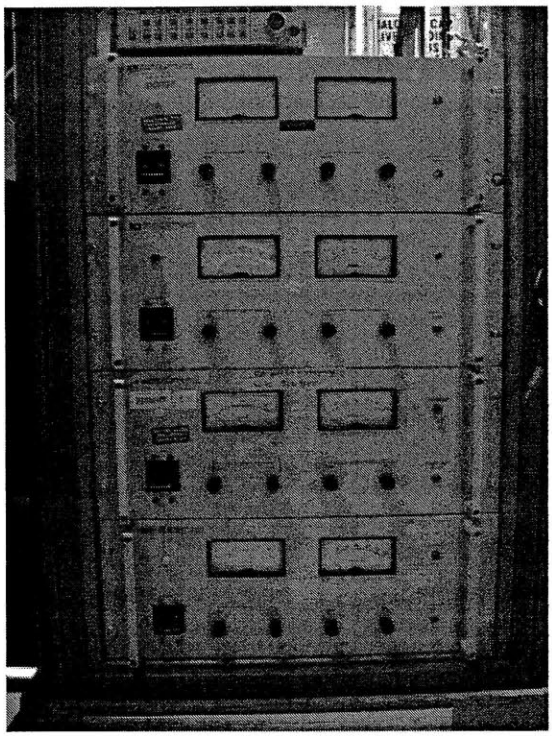

Figure 3-8: HP power supplies used to charge the sample coils.

The JASTEC magnet was charged by an Oxford model IPS 125-9 power supply. It was the same power supply used in short sample tests. The sample coils were charged by a series of HP power supplies, as shown in Figure 3-8. They were connected in parallel and controlled in master and slave mode. All of them were controlled remotely by inputting a voltage. The voltage was generated by an SCIX card, which was in turn controlled by a desktop computer. Each of the power supplies could output up to 120 A current, with the voltage compliance of 12 V. All the modules together could provide up to 480 A.

3.1.4 Data Acquisition System

In the coil tests, collected signals included: temperatures, current applied to the coil, voltage across the coil, magnetic field measured by Hall sensor and liquid helium level measured by a liquid helium level meter. Since, in the coil tests, background fields were kept at constant values, there was no need to collect this information. The field

could be read out directly from the Oxford power supply.

Temperatures were measured by Cernox™ sensors at three locations. One sensor was attached at the top of the coil, one was attached at the bottom of the coil, and the third was attached outside the wall of the copper can. The three sensors together were used to make sure the temperature was uniform in the can and in the coil.

As with the short sample tests, current applied to the coils also passed a shunt resistor. The voltage across the shunt resistor was collected and recorded. This voltage was proportional to the current.

A Hall sensor was used to measure the magnetic field generated by the sample coils.

Voltage across the shunt, voltage across the coil, and voltage of Hall sensor were collected by SCIX data acquisition system and then stored in a desktop computer.

A liquid helium level meter was installed on the side of the aluminum chamber. It could tell the level of liquid helium in the cryostat during the tests conveniently. A liquid helium level meter is made of a piece of NbTi wire. The wire is electrified when measuring; if part of the wire is in liquid helium, that part becomes superconducting. The level can then be told from the resistance of the wire. Because the level meter boils liquid helium when measuring, it was only turned on when we wanted to know the level of liquid helium.

3.2 Experimental Design

3.2.1 Design of Coils

A 100-m multifilament MgB_2 coil, a 100-m monofilament MgB_2 coil, and a 100-m monofilament NbTi coil were wound and tested. The designed geometric and electric properties of the coils are listed in Table 3.1.

I.D.	O.D.	Height	Turns	Center Field	Inductance
31.8 mm	49.0 mm	76.2 mm	750	1.1 T per 100 A	8.2 mH

Table 3.1: Geometric and electric properties of the 100-m coils.

3.2.2 Design of Current Lead Connectors

A pair of copper pieces were made to connect the leads of the MgB_2 coils to the current leads. They were designed in such a way that two of them formed a cylinder which almost blocked the hole on the cap of the aluminum chamber and the hole through the styrofoam in the chamber. This helped keep the inside of the chamber an isolated space, and a relatively higher pressure could be built inside the chamber when the heater vaporized the liquid helium. The helium vapor had a hard time getting out, so the pressure was built. The higher pressure could stop liquid helium seeping into the chamber from outside, when the heater was turned on. This delicate design could save liquid helium and reduce the required power of the heater. A single copper piece was designed to fit a piece of MgB_2 wire, a piece of YBCO tape, and two pieces of NbTi conductor at the same time perfectly. The MgB_2 wires came from the coil and the other conductors were connected to the current leads. They were soldered together in the connectors and the whole thing formed a solid piece. The two connectors were insulated by Kapton tape inbetween them. Figure 3-9 shows the connectors when they were installed.

3.2.3 Purposes of the Tests

100-m Multifilament MgB_2 Coil

The purposes of testing a 100-m multifilament MgB_2 coil were:

- To prove that the MgB_2 wire with this cross section area has a critical current high enough to build an MRI magnet.
- To be compared with monofilament MgB_2 coil, proving that monofilament MgB_2 coil performs as good as multifilament MgB_2 coil, in terms of critical current.

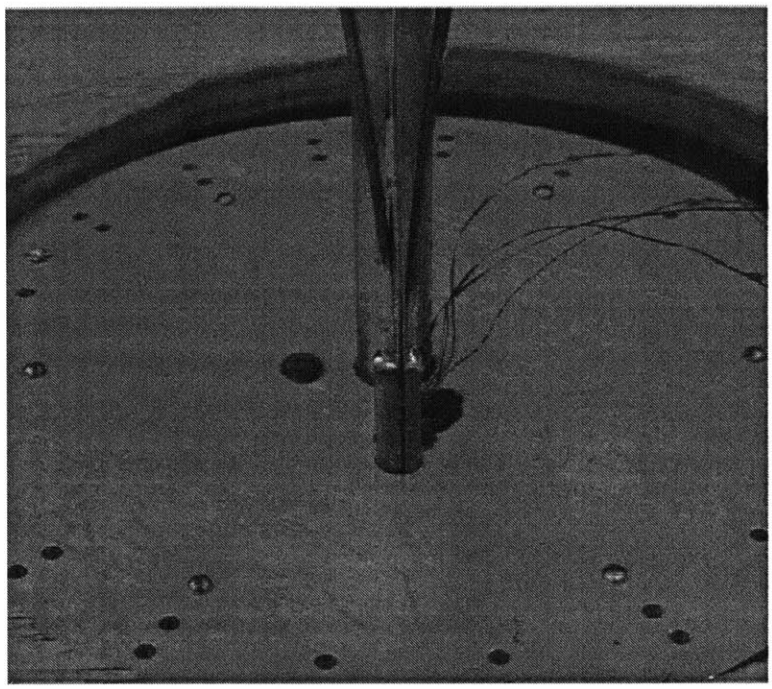

Figure 3-9: The assembled connectors through the hole of the aluminum chamber.

100-m Monofilament MgB_2 Coil

The purposes of testing a 100-m monofilament MgB_2 coil were:

- To prove that the monofilament MgB_2 wire is suitable for a 0.5 T MRI magnet.
- To prove that the monofilament MgB_2 wire does not have flux jumping, or flux jumping does not lead to premature quench.
- To test the comprehensive performance of the monofilament MgB_2 wire in a coil, including stability, reliability and strength.

100-m Monofilament NbTi Coil

The purposes of testing a 100-m monofilament NbTi coil were:

- To prove that the monofilament NbTi wire has flux jumping which is stronger than MgB_2.

- To prove the entire test design is correct by showing that the monofilament NbTi coil has serious flux jumping. Thus the results of the monofilament MgB_2 coil is reliable.

3.2.4 Test Plans

100-m Multifilament MgB_2 Coil

The tests of the 100-m multifilament MgB_2 coil included:

1. Measure the critical currents of the coil in different background magnetic field.
2. Measure the critical currents of the coil at different temperatures, ranging from 4.2 K to 15 K.

100-m Monofilament MgB_2 Coil

The tests of the 100-m monofilament MgB_2 coil included:

1. Measure the critical currents of the coil in different background magnetic field, especially in 1 T background field and in self-field.
2. Measure the critical currents of the coil at different temperatures, ranging from 4.2 K to 15 K.
3. Test the sturdiness of the monofilament MgB_2 wire when the coil quenches.
4. Test the stability of the coil at different ramping rates.
5. Test the reliability of the coil by charging the coil multiple times.

100-m Monofilament NbTi Coil

The critical current of the monofilament NbTi wire is very high. At 4.2 K and in 3 T background magnetic field, the critical current of a commercial Φ0.7 mm monofilament NbTi wire made by Supercon is 250 A [23]. As to our tests, we used a spool of specially fabricated Φ0.8 mm monofilament NbTi wire. In low background

field where flux jumping happens, the critical current of the wire would no doubt far exceed 300 A. With this conductor, even a premature quench happened at 50% critical current could burn the coil. So, our tests of the 100-m monofilament MgB_2 coil focused on the stability of the coil at different ramping rates. We did not try to measure the critical current of the coil.

3.3 Experimental Procedures

3.3.1 Coil Preparation

Coil Forms

The forms of the coils were designed in such a way that the entire coil, including the coil form, can be heat treated up to 700 C in furnace. The top pieces and bottom pieces were separately machined out of 1/4-inch thick stainless steel plates; the mandrels were cut from a Φ1 1/4-inch stainless steel tube. The three pieces were assembled and welded in the Central Machine Shop at MIT.

A slot and an indent were machined on the top piece in order to let two leads come out. A coil form with wound coil is shown in Figure 3-10.

Coil Winding

The 100-m coils were wound by a winding machine, as shown in Figure 3-11. It was taken when the 100-m monofilament MgB_2 coil was being wound. Both the multifilament and monofilament MgB_2 wires were purchased from Hyper Tech Research, Inc. The monofilament MgB_2 wire was the same as the wire used in the short sample tests. The monofilament NbTi wire was purchased from Surpercon, Inc. Different from the NbTi wire used in the short sample tests, this wire was insulated by formvar.

When the winding was finished, before the tension could be released from the wire and the coil could be taken off the winding machine, the last few turns of the coil must be fixed. The fixture must endure the heat treatment at 700 C with the coil. One way to fix the coil was to wrap a few turns of copper or stainless steel wire at

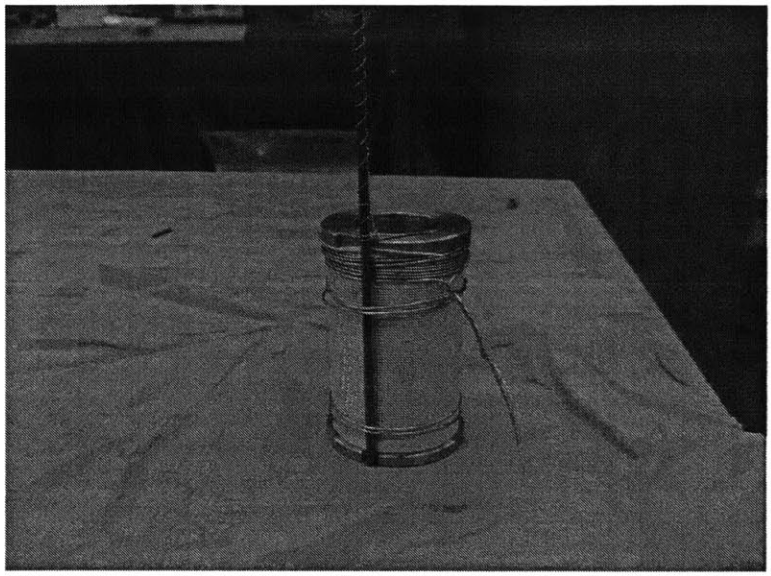

Figure 3-10: A wound 100-m MgB_2 coil before heat treatment. A few turns of stainless steel wire was wrapped to tighten the winding. The leads of the coil were tied on a stainless steel rod to avoid bending during heat treatment.

the end of the coil.

Heat Treatment

After winding, MgB_2 coils must be heat treated in the furnace. The temperature profile for heat treating MgB_2 coils was the same as for MgB_2 short samples. Because once MgB_2 wire is heat treated, it becomes brittle and delicate, the two leads of the coil were tied on a stainless steel rod in order to be kept straight during the heat treatment, as shown in Figure 3-10.

3.3.2 Test Operations

Pre-Cooling

To begin the test, we first placed the cryostat in the bore of the JASTEC magnet. After it was settled, we started to cool the cryostat with liquid nitrogen. This step was to cool the shield of the cryostat, which is required for liquid helium tests. Then we pre-cooled the sample container in liquid nitrogen. When pre-cooling finished, the

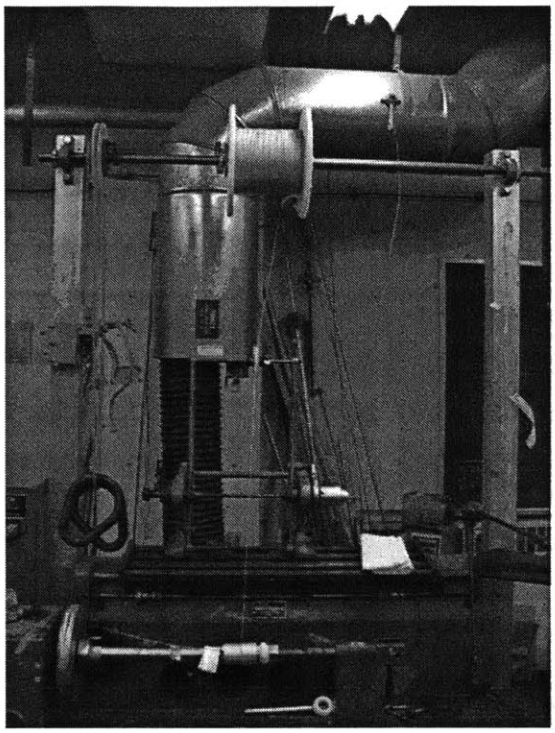

Figure 3-11: The winding machine used to wind all the 100-m sample coils.

sample container assembly was inserted in the cryostat. Then all the signal wires were connected to the monitors and data acquisition system.

Liquid Helium Transfer

To further cool the sample assembly, liquid helium was transferred from the liquid helium dewar to the cryostat.A vacuum transfer line was used to transfer liquid helium, as shown on the top of Figure 3-12. Both sides of the transfer line should be inserted to the very bottom. On the liquid helium dewar side, the transfer line should reach the bottom in order to transfer as much liquid helium as possible. On the cryostat side, the transfer line should reach the bottom so that the liquid helium was first filled to the bottom of the sample assembly. Even when the helium was vaporized, the remainder of the assembly could still be cooled by cold gas helium. This is the most efficient way to use liquid helium for cooling.

To start the transfer, we connected the liquid helium dewar to a high pressure

helium column. By controlling the pressure that the column applied to the dewar, we were able to control the transfer rate. The bottom of Figure 3-12 shows the connection between the high pressure helium column and the liquid helium dewar.

The maximum level of liquid helium was determined by the position of shields. The level should not be too high; otherwise, it would evaporate too fast. The minimum level of liquid helium was determined by the height of the coil. The level should be high enough in order to maintain an isothermal environment in the copper can. During the experiment, we monitored the level of liquid helium regularly. Once the level fell below the minimum level, we had to stop the test and refill liquid helium through transfer line.

Temperature Control

The heater was powered by an HP Harrison 6200B power supply. The output of the power supply could be adjusted very accurately. When the coil was in the helium environment, we could control the output of the power supply manually to find a balance between heating of the heater and cooling of helium. It was not difficult to find the balance and keep the temperature constant for a few minutes. This period was long enough to finish a test.

3.4 Results and Discussions

3.4.1 Critical Current Comparison Between Multifilament and Monofilament MgB_2 Coils

Figure 3-13 shows the critical currents of the 100-m multifilament MgB_2 coil, from 4.2 K to 15 K, in 1 T background field and self-field. Figure 3-14 shows the critical currents of the 100-m monofilament MgB_2 coil measured in the same conditions.

At 4.2 K, in self-field, the multifilament coil had a critical current slightly over 200 A. In the same condition, the monofilament coil had a critical current of 200 A. At 15 K, in self-field, at which condition our future MgB_2 MRI magnet is supposed

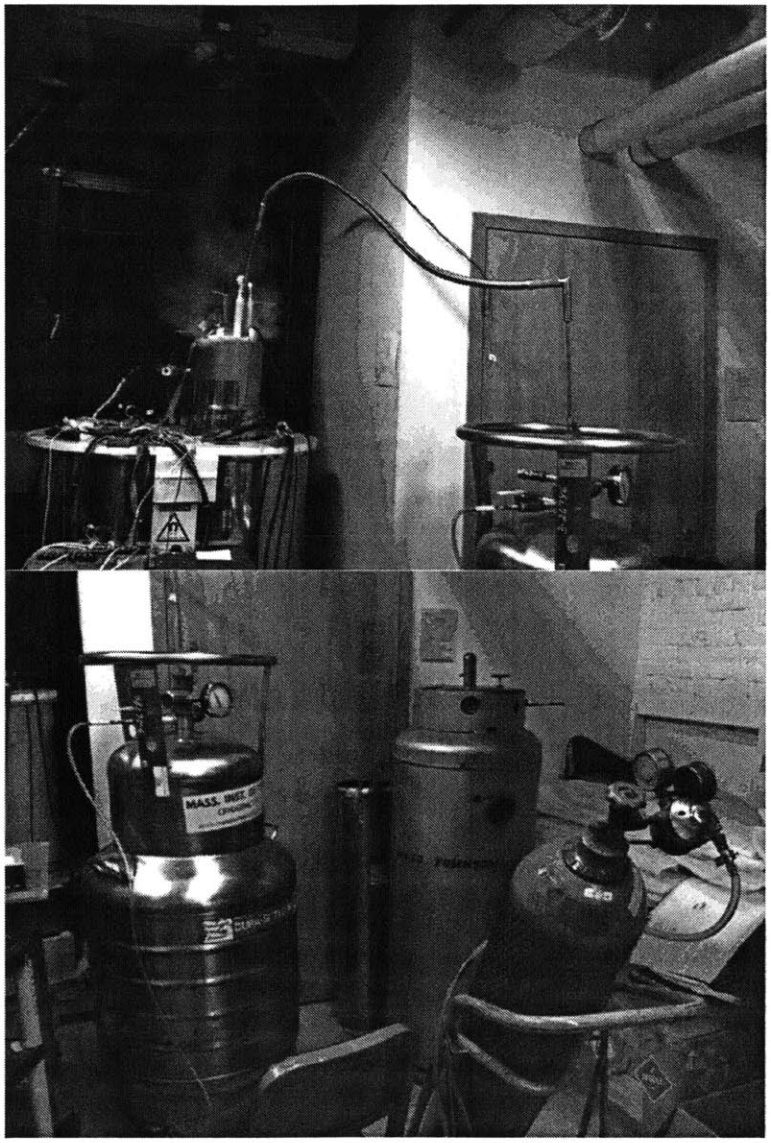

Figure 3-12: Liquid helium transfer. On the top, liquid helium was being transferred from the liquid helium dewar to the cryostat through a transfer line. On the bottom, a high pressure helium column was giving pressure to the liquid helium dewar.

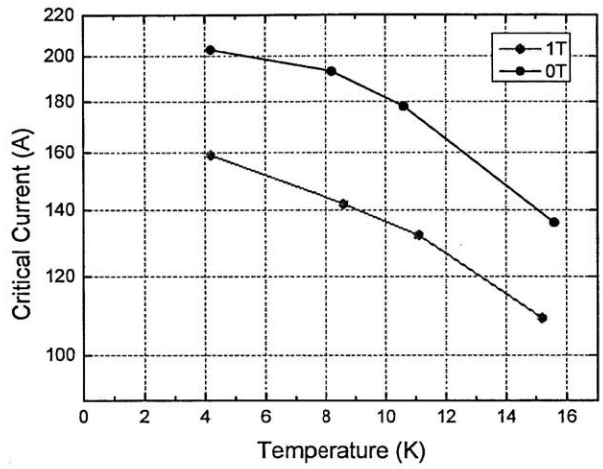

Figure 3-13: Critical currents of the 100-m multifilament MgB_2 coil, from 4.2 K to 15 K, in 1 T background field and self-field.

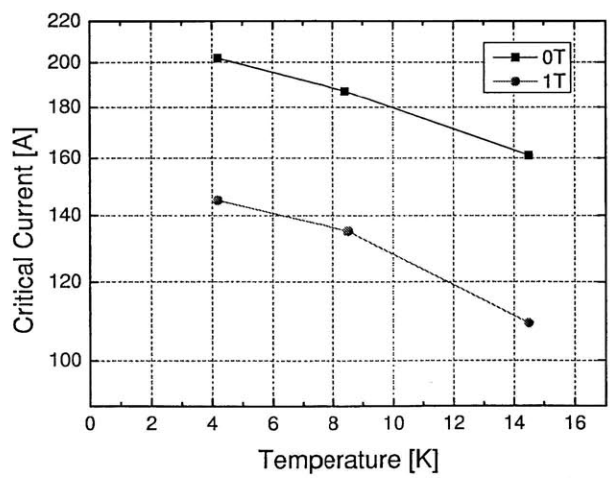

Figure 3-14: Critical currents of the 100-m monofilament MgB_2 coil, from 4.2 K to 15 K, in 1 T background field and self-field.

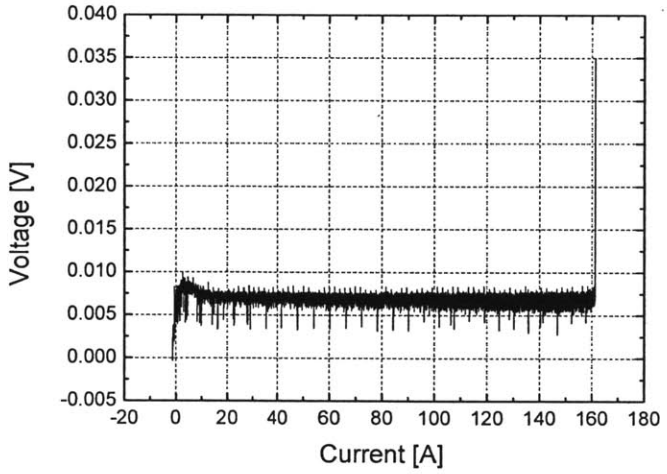

Figure 3-15: A voltage vs. current graph of monofilament MgB_2 coil. The horizontal axis is the transport current in [A]. The vertical axis is the voltage across the coil in [V]. The steep increase of the voltage indicates a quench at critical current. The coil survived from such quenches for multiple times.

to work, the multifilament coil had a critical current of 138 A, but the monofilament coil had a critical current of 160 A. The self-field here was about 1.5 T for both coils. This means for MRI magnets smaller than 1.5 T, monofilament MgB_2 wire is possibly more appropriate than multifilament MgB_2 wire, at least in terms of critical current.

Usually a more important characteristic of wire is critical current density. Because monofilament MgB_2 wire has a superconducting cross section area almost 3 times of that of multifilament MgB_2 wire, the critical current density of monofilament MgB_2 is still lower than multifilament one. However, in magnets, the overall ampere-turn is most important, so the comparison here in critical current makes some sense. So, in terms of critical current, monofilament MgB_2 wire is a good option for MRI magnets.

3.4.2 Quench Safety at Critical Current

Figure 3-15 shows a typical voltage vs. current curve when the monofilament MgB_2 coil was charged. The horizontal axis is transporting current in [A]. The vertical axis is the voltage across the coil in [V]. On the right end of the curve, the steep increase of voltage indicates a quench at critical current happened. Right after the quench, the

current was reduced to zero immediately at 5 A/s. This operation was done manually, so the response time was about 0.3~0.4 second.

At the moment, some zone in the winding reached the critical current first and turned into normal state. These zones usually are located at the center of the innermost layer or where the wire is weaker due to defects. Because the current was very high, a huge amount of magnetic energy was released in terms of Joule heat in these zones. In some cases, the heat cannot be conducted away fast enough so that the wire in the zones could be burnt. During the tests, the coil quenched a few times at critical current and it survived from all of them. This shows that the monofilament MgB_2 wire is sturdy enough to withstand a quench. In real magnets, with proper quench detection and protection mechanism, people should be able to protect the wire from being burnt.

3.4.3 Kaiser Effect: No Mechanical Disturbance

When the monofilament MgB_2 coil was being charged, the voltage signal was not very smooth, as shown in Figure 3-15. This means that there were disturbances during the charging period. It was highly possible that this caused by flux motion; however, mechanical disturbances, such as wire movement, could also cause this kind of fluctuation. In order to exclude the possibility of mechanical movement, we made use of the Kaiser effect to justify.

Kaiser effect says that if the voltage fluctuation is solely caused by mechanical movement, the voltage curve should be flat after the first charging unless the coil is charged to a higher magnitude. Due to Kaiser effect, if the voltage fluctuation came from mechanical movement, we should be able to observe a quiet segment at the beginning of the second charging.

Following this idea, we charged the coil from virgin state to different magnitude at a constant ramping rate of 1 A/s, at 4.2 K, in 2 T background field. We first charged the coil up to 10 A. We discharged the coil back to 0 and then charged it up to 20 A. We then repeated the process once more and charged it up to 40 A. The voltage vs. current curves are shown in Figure 3-16. From the graphs, we can clearly

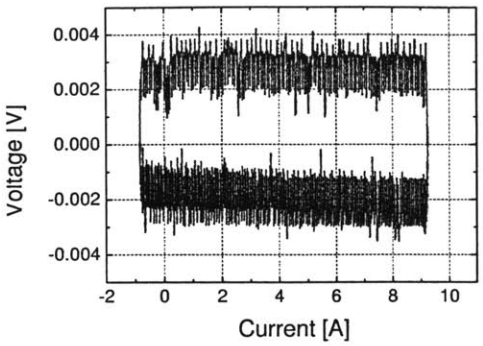

(a) Charged the coil up to 10 A.

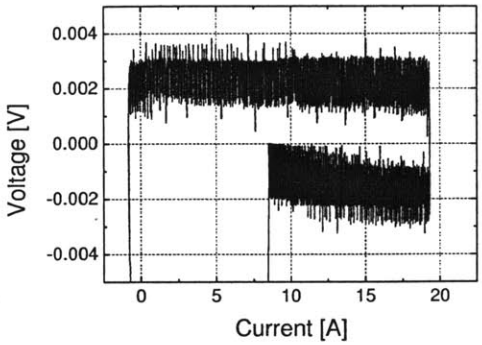

(b) Charged the coil up to 20 A.

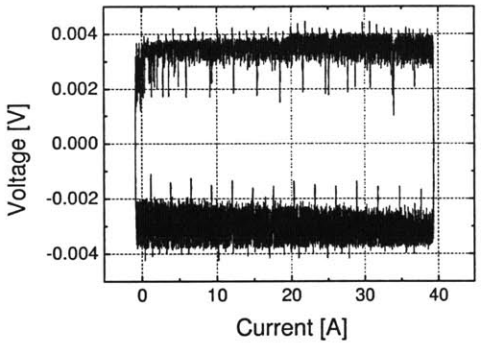

(c) Charged the coil up to 40 A.

Figure 3-16: Voltage vs. current curves of charging the monofilament MgB_2 coil up to different currents in sequence. Charging current started from low to high. None of the curves started with a quiet section.

see that voltage fluctuated from the very beginning during all the charting processes. The noise of the curve was not better at all for the second or third charging. These tests demonstrate that the voltage fluctuation did not, at least did not solely come from mechanical movement; the noise had to do something with flux motion.

3.4.4 Partial Flux Jumping

The voltage vs. current curve of monofilament MgB_2 coil is noisy during both charging and discharging period. From previous argument, we expected that the noise and the large spikes came from flux motion. In order to justify this fact and see the effect of flux motion on the coil, we charged the coil with different ramping rates, e.g., at 1

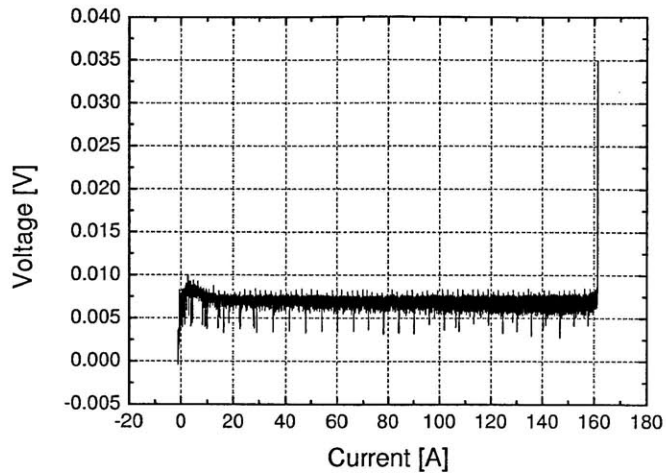

Figure 3-17: The voltage vs. current curve when the monofilament MgB_2 coil was charged at 1 A/s. The coil quenched at critical current.

A/s, 2 A/s and 5 A/s respectively. The time varying current generates Joule heat in type II superconductors due to "AC loss". The higher ramping rate means a faster time-varying current, which generates heat with a higher power. The heat will cause a perturbation in the superconductor and possibly induce flux jumping. The higher ramping rate is more likely to induce flux jumping. So, we tested the coil at different ramping rates to see if there would be any difference in the curves. We expected larger spikes would occur in higher ramping rate tests.

Because the MgB_2 MRI magnets are eventually supposed to work at 15 K, in self-field, the series of ramping rate tests were done at 15 K and in self-field too.

Effects of Ramping Rate

From Figure 3-17 to Figure 3-19, we can find a trend that the spikes were getting larger and more periodic when the ramping rates were higher. In Figure 3-17, most of the spikes were in the range of 0.0025 V to 0.0075 V; the strengths of the spikes were within 0.005 V. In Figure 3-18, the spikes were in the range of 0.01 V to 0.015 V; the strengths of the spikes were also within 0.005 V. Although the strengths of the spikes were not higher, the spikes did show a clearer pattern of period. The periodic

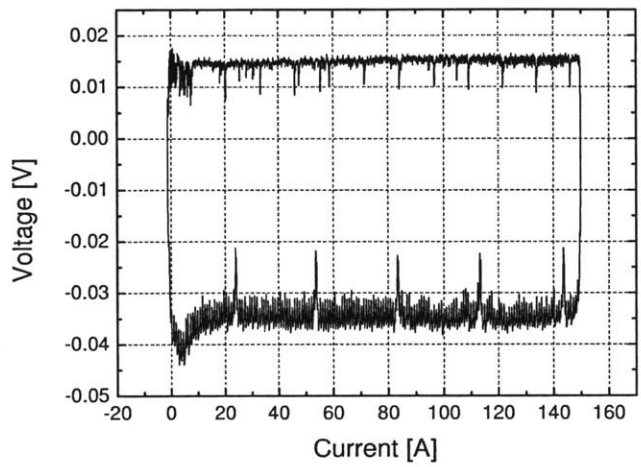

Figure 3-18: The voltage vs. current curve when the monofilament MgB_2 coil was charged at 2 A/s. The coil was discharged at 5 A/s.

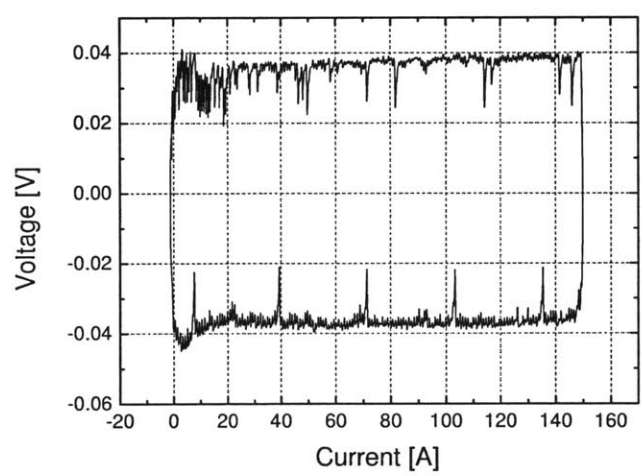

Figure 3-19: The voltage vs. current curve when the monofilament MgB_2 coil was charged at 5 A/s. The coil was discharged at 5 A/s.

pattern of the spikes was most obvious in Figure 3-19, when the ramping rate was 5 A/s. The strengths of the large spikes were about 0.02 V, almost 4 times of the strength of spikes when the ramping rate was 1 A/s.

A first conclusion can be drawn here that higher ramping rate does induce stronger flux motion because the spikes are stronger. The shape of the spikes is very similar to the shape of a magnetization trace which having flux jumping teeth; although the spikes here are directly measured in voltage. In addition, the spikes have a very clear periodic tendency. All of these evidences show that flux jumping happened in the monofilament MgB_2 coil.

Cause of the Voltage Fluctuation

The spikes were measured in voltage; it is not very obvious how the voltage was connected with magnetization and flux motion.

For a coil we have

$$V = L\frac{dI}{dt} \tag{3.1}$$

where V is the voltage across the coil, L is the inductance of the coil, and I is the current flowing in the coil.

From Equation 3.1 we know that the voltage across the coil is directly proportional to rate of change in current. We can check the current in the coil to see if it coincided with the voltage.

Figure 3-20 shows the current and voltage vs. time curves in the same graph. The horizontal axis is the test time in [s]. The left vertical axis is the current flowing in the coil in [A]. The right vertical axis is the voltage across the coil in [V]. Figure 3-21 shows a zoomed-in section of the curves where the voltage has a spike. Obviously, corresponding to the voltage, the ramping rate of the current is also slower than the other section. A further calculation shows the relation more clearly. Figure 3-22 shows the curve of differentiated current timing the inductance of the coil. When doing the differentiation, Savitzky-Golay smooth was employed to get a smoother

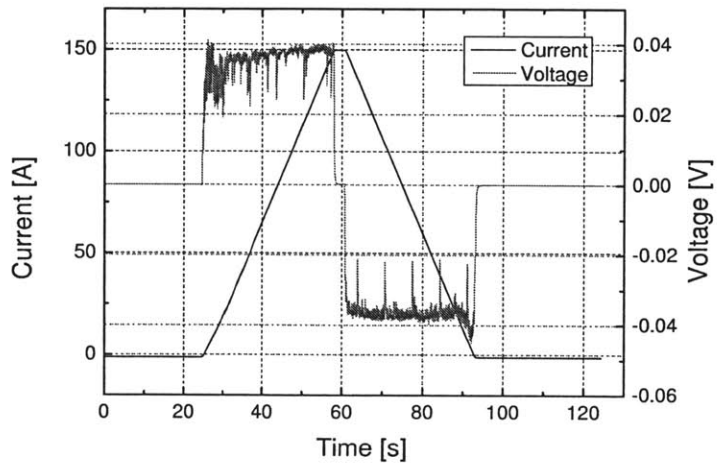

Figure 3-20: Current and voltage vs. time curves. The horizontal axis is the test time in [s]. The left vertical axis is the current flowing in the coil in [A]. The right vertical axis is the voltage across the coil in [V].

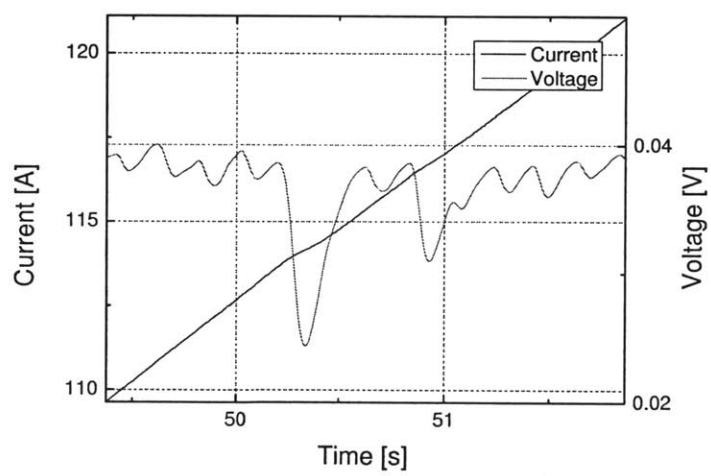

Figure 3-21: Zoomed-in current and voltage vs. time curves. Where the voltage has a spike, the varying rate of current is slower.

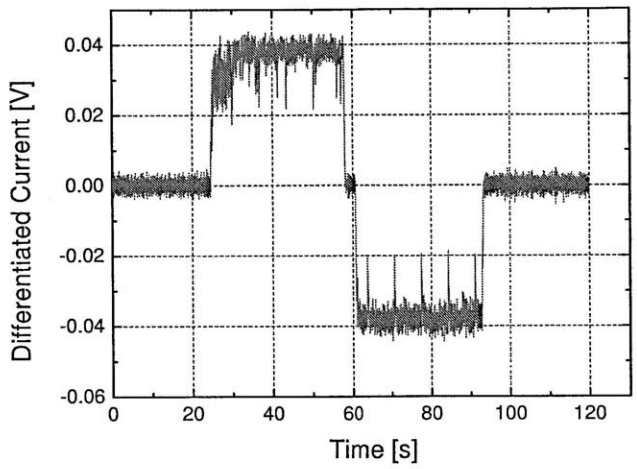

Figure 3-22: The curve of differentiated current timing the inductance of the coil. It is in the unit of [V].

curve. Comparing this curve with the voltage curve in Figure 3-20, we can see a perfect match of the curves, in terms of both the magnitude and the pattern.

When there was a flux jumping happened somewhere in the coil, the motion of the flux gave a resistance to the power supply, which caused the ramping rate decreasing at that moment. The decreased ramping rate, in turn, lowered the voltage across the coil. This was how the flux motion caused the voltage fluctuation.

In the tests, the spikes were still small compared to the charging voltage of the coil. If the flux jumping happened, it must be a partial flux jumping which happened in a local zone. Otherwise, it would cause a much stronger spike in voltage; the bottom of the spike could reach 0. Besides, the ramping rate of the current went back to set value soon; the spikes in voltage were very narrow. They showed that the flux jumping recovered soon after it happened.

So, the measured voltage demonstrated that there could be flux motion in the monofilament MgB_2 coil; but even if it was flux jumping, it must be local partial flux jumping which recovered soon.

3.4.5 Premature Quench

Although the ramping rate tests demonstrated the existence of flux jumping in monofilament MgB_2 coil, we care more about the consequence of flux jumping rather than flux jumping itself. The only concern we have with flux jumping is whether flux jumping in the superconductor would cause a premature quench of the coil. This was the reason why early monofilament superconducting magnets failed in 1960s.

In order to justify the effects of flux jumping to the coil, we charged the monofilament MgB_2 coil up to 150 A several times at 5 A/s, which is 90% of the critical current at 15 K, in self-field. As shown in Figure 3-19, all the tests ended when the coil was still superconducting; in none of the tests did we observe premature quench. Since real MRI magnets work at no more than 90% of their critical currents, the flux jumping issue would likely not lead to premature quench at that current level.

In addition, for real MRI magnets, the ramping rate of current is usually of the order of 0.01 A/s, which is far slower than the ramping rate tested in these tests. Monofilament MgB_2 MRI magnets should be even safer.

So, although the monofilament MgB_2 coil has flux jumping, flux jumping does not induce premature quench, even in the extreme case that the current ramped up to 90% of its critical value at a rate 100 times faster than real MRI magnets.

3.4.6 Flux Jumping in Monofilament NbTi Coil

In order to justify the results of the above tests were reliable, we tested a monofilament NbTi coil in the similar way. The coil was tested at 4.2 K, in 2 T background field. We ramped the coil at 0.5 A/s and 1 A/s, and the voltage vs. current curves are shown in Figure 3-23.

The top picture of Figure 3-23 shows the voltage vs. current curve measured when the coil was charged at 0.5 A/s, while the bottom one shows the curve measured at 1 A/s. In both tests the coil was charged up to about 10 A. At these ramping rates and the current level, we can observe spikes that were similar to those observed in the monofilament MgB_2 coil. However, in monofilament NbTi coil, the spikes were

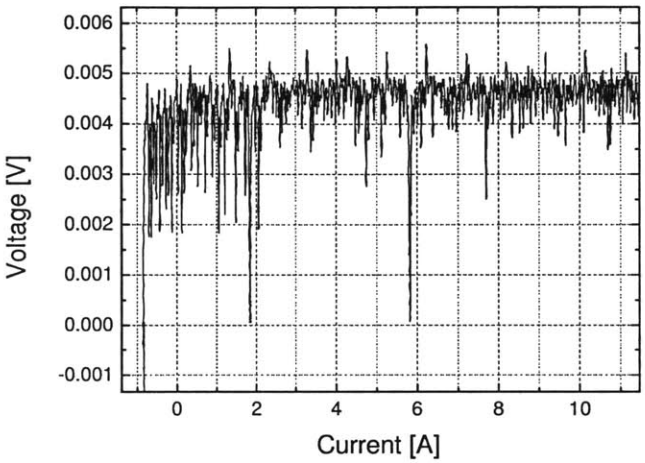

(a) Energize the coil at 0.5 A/s.

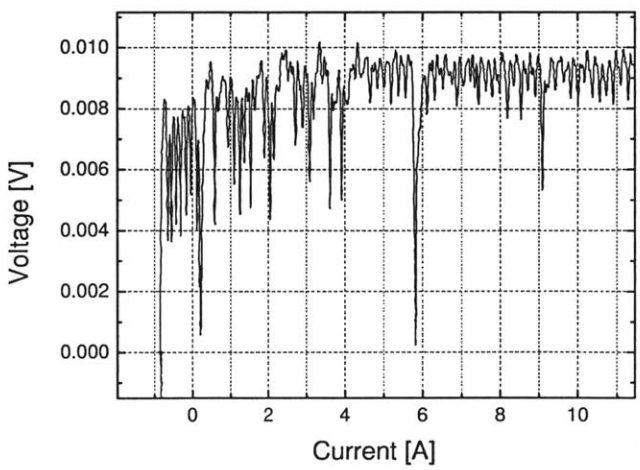

(b) Energize the coil at 1 A/s.

Figure 3-23: Voltage vs. current curves of energizing the monofilament NbTi coil at 0.5 A/s and 1 A/s. Spikes were deep and almost down to 0.

deeper, and the tips of the spikes were almost down to 0. This was a direct indication of flux jumping. In the tests, the flux jumping did not give rise to a premature quench, because the current level was very low; but, if the same flux jumping happened at higher current level, it would very likely induce quenches.

Since the monofilament NbTi coil had stronger flux jumping than monofilament MgB_2 coil, our test results were proved to be reliable.

Chapter 4

Conclusions

In the short sample tests, we measured the magnetization trace of the short samples of monofilament MgB_2 wire and monofilament NbTi wire. From the magnetization traces, we have seen insignificant flux jumping in short samples of monofilament MgB_2 wire. Compared with the trace of monofilament NbTi, the trace of MgB_2 was smooth. So we could expect that in 100-m coil tests, monofilament MgB_2 coil would perform well.

In the 100-m coil tests, we tested the monofilament MgB_2 coil in many ways to insure flux jumping would not be an issue. The critical currents at different temperatures and in different fields were measured; they were proved to be essentially the same as those of the multifilament MgB_2 coil. In the tests, we did observe some fluctuation in the voltage across the coil, and we discussed that it came from the flux motion in the coil. However, we succeeded to show that these flux motions did not induce premature quench. We energized the monofilament MgB_2 coil at different ramping rates, and the coil survived in all the tests, up to 90% of its critical current. The coil tests showed directly that the monofilament MgB_2 wire is immune to premature quench and thus good for magnet applications.

Since we have developed a reliable superconducting joints technology which uses monofilament MgB_2 wire, we are able to build persistent-current mode MgB_2 magnets. In the future, we will test a persistent-current mode coil of monofilament MgB_2 to further justify our integrated technologies, before we build a whole-body MRI magnet

with monofilament MgB_2 wire in the end.

Bibliography

[1] H. K. Onnes. Investigations into the properties of substances at low temperatures, which have led, amongst other things, to the preparation of liquid helium. Nobel Lecture, Dec 1913.

[2] M. N. Wilson. 100 years of superconductivity, 50 years of superconducting magnets. MT-22 Conference Talk, Sep 2011.

[3] S. Hahn. Superconducting technology for high field and large power applications. Presentation, March 2012.

[4] Z. H. Cho. `http://blog.yonhapnews.co.kr/scoopkim/post/101053/`, 2006.

[5] Y. Iwasa. Superconducting magnet technology: An introduction. Presentation at Tsinghua University, Apr 2009.

[6] D. K. Park, J. Ling, M. Rindfleisch, and et al. MgB_2 for mri magnets: Test coils and superconducting joints results. *IEEE Transactions on Applied Superconductivity*, 22(3), Jun 2012.

[7] Y. Iwasa. *Case Studies in Superconducting Magnets: Design and Operational Issues.* Springer, second edition edition, 2009.

[8] M.D. Sumption, E.W. Collings, E. Lee, X.L. Wang, S. Soltanina, S.X. Dou, , and M.T. Tomsic. Real and apparent loss suppression in mgb2 superconducting composite. *Physica C*, 98, 2002.

[9] B. T. Matthias, T. H. Geballe, S. Geller, and et al. Superconductivity of nb3sn. *Physical Review*, 95(6):1435–1435, 1954.

[10] J. G. Bendnorz and K. A. Müller. Possible high tc superconductivity in the ba-la-cu-o system. *Zeitschrift Für Physik B - Condensed Matter*, 64(2):189–193, 1986.

[11] H. Maeda, Y. Tanaka, M. Fukutomi, and et al. A new high-tc oxide superconductor without a rare-earth element. *Japanese Journal of Applied Physics Part 2-Letters*, 27(2):L209–L210, 1988.

[12] M. K. Wu, J. R. Ashburn, C. J. Torng, and et al. Superconductivity at 93-k in a new mixed-phase y- ba-cu-o compound system at ambient pressure. *Physical Review Letters*, 58(9):908–910, 1987.

[13] J. Nagamatsu, N. Nakagawa, T. Muranaka, and et al. Superconductivity at 39 k in magnesium diboride. *Nature*, 410(6824):63–64, 2001.

[14] Y. Iwasa, J. Bascunan, S. Hahn, and D. Park. Personal conversations.

[15] Wikipedia. Magnetic resonance imaging. `http://en.wikipedia.org/wiki/Magnetic_resonance_imaging`.

[16] T. C. Cosmus and M. Parizh. Advances in whole-body mri magnets. *IEEE Transactions on Applied Superconductivity*, 21(3), Jun 2011.

[17] S. Hahn. Personal communication.

[18] S. Hahn. Personal conversation.

[19] J. L. Ackerman. Personal Communication on 15-T/133-mm Open MRI Magnet Quench at Massachusetts General Hospital, Dec 2010.

[20] Y. Iwasa. Hts magnet activities for nmr and mri at m.i.t. francis bitter magnet laboratory. Presentation at Tsinghua University, Apr 2009.

[21] W. Yao, J. Bascunan, S. Hahn, and Y. Iwasa. A superconducting joint technique for MgB_2 round wires. *IEEE Transactions on Applied Superconductivity*, 19(3), Jun 2009.

[22] N. W. Martin. *Superconducting Magnets*. Oxford University Press, 1987.

[23] Supercon Inc. Standard nbti supercon conductors. `http://www.supercon-wire.com/products_nbti.html#MonoTable`.